Essential role of the C148 – C227 disulphide bridge in the human 5-HT_{2A} homodimeric receptor

Cimadevila M[1], Gómez-García L[1], Martínez AL[1], Iglesias A[1,2], López-Giménez J[3], Castro M[4], Cadavid MI[1], Loza MI[1*], Brea J[1]**

[1]BioFarma Research Group, Centro Singular de Investigación en Medicina Molecular y Enfermedades Crónicas (CIMUS), Universidade de Santiago de Compostela, Santiago de Compostela, Spain

[2]Current position at Laboratory of Epigenomics in Endocrinology and Nutrition, Fundación Instituto de Investigación Sanitaria de Santiago de Compostela (FIDIS). Complejo Hospitalario Universitario de Santiago de Compostela (CHUS/SERGAS), Santiago de Compostela, Spain

[3]Instituto de Parasitología y Biomedicina "López-Neyra" IPBLN-CSIC. Av/ del Conocimiento, 17. 18016 Granada -- Institute of Parasitology and Biomedicine "López-Neyra" (IPBLN-CSIC), Armilla, 18016, Granada, Spain

[4]Department of Pharmacology, Centro Singular de Investigación en Medicina Molecular y Enfermedades Crónicas (CIMUS), Universidade de Santiago de Compostela, Santiago de Compostela, Spain

*corresponding author. E-mail: mabel.loza@usc.es

**corresponding author. E-mail: pepo.brea@usc.es

Abstract

The 5-HT_{2A} receptor is a homodimeric G protein-coupled receptor implied in multiple diseases, including schizophrenia. Recently, its co-crystallisation with the antipsychotic drugs zotepine and risperidone has revealed the importance of its extracellular domains in its pharmacology. Previous studies have shown that the non-specific disruption of extracellular

disulphide bridges in the 5-HT_{2A} receptor decreases ligand binding and receptor activation. There is enough evidence to hypothesize that this decrease may be due to a reduction of the disulphide bridge that links transmembrane domain 3 (TM-3) and extracellular loop 2 (ECL-2) of the 5-HT_{2A} receptor via cysteine 148 (C148) and C227.

Thus, to study the influence of the C148 – C227 disulphide bridge on 5-HT_{2A} receptor pharmacology, we substituted C148 and C227 in the human 5-HT_{2A} receptor (WT) with alanines, to obtain two single mutants (C148A and C227A) and a double mutant (C148A/C227A), and the resultant DNA constructs were used to generate four stable cell lines. These substitutions reduced the binding of the 5-HT_{2A} receptor to [^{3}H]lysergic acid diethylamide ([^{3}H]LSD) and impeded the 5-HT_{2A} receptor-mediated activation of phospholipase C (PLC). Furthermore, bioluminescence resonance energy transfer (BRET) and western blotting analysis revealed that these mutations did not alter the homodimeric nature of the 5-HT_{2A} receptor. However, fluorescence microscopy showed that these mutations hindered receptor trafficking to the cell membrane.

These results illustrate the importance of the disulphide bridge between TM-3 and ECL-2 in maintaining the correct 5-HT_{2A} receptor conformation to allow ligand binding and migration of the homodimeric receptor to the cell membrane.

Keywords

Serotonin 2A receptor; GPCRs; extracellular domains; disulfide bridge; ligand binding

1. Introduction

The serotonin 2A receptor (5-HT_{2A}), a G protein-coupled receptor (GPCR), is implicated in the pathogenesis of multiple diseases, such as schizophrenia (1). Antagonism of this receptor is part of the mechanism of action of the majority of antipsychotic drugs used in therapeutic practice today, because it contributes to alleviate the negative symptoms of the disease (2,3). Therefore, there is a necessity to elucidate the complex pharmacology of the 5-HT_{2A} receptor.

From a functional point of view, the 5-HT_{2A} receptor activates phospholipase C (PLC) through a G_q protein, leading to the intracellular release of inositol phosphate species (IPs), which act as second messengers. Apart from PLC activation, the 5-HT_{2A} receptor stimulates $G_{12/13}$ proteins to release arachidonic acid (AA) into the extracellular space. Interestingly, the 5-HT_{2A} receptor was among the first receptors for which functional selectivity was described (4). Functional selectivity is the process by which a ligand stabilises the different conformations of a receptor to allow the subsequent activation of different intracellular pathways (5).

Similar to other GPCRs, the 5-HT_{2A} receptor is reported to form homodimers which are the minimal functional unit for both IPs and AA pathways (7-9). Moreover, this receptor also forms heterodimers with the dopamine 2 (D_2) receptor (8), the cannabinoid 1 (CB_1) receptor (9), the serotonin 1A (5-HT_{1A}) receptor (10), and the glutamate 2 (mGlu2) receptor (11–13). These oligomers have emerged as novel therapeutic targets that can be specifically manipulated to treat different diseases as their properties differ from their monomeric counterparts (14–18).

Although a vast amount of literature is dedicated to it, the molecular basis of 5-HT_{2A} receptor activation remains unknown, restricting the development of more effective drugs. Targeting the 5-HT_{2A} receptor is now easier due to the availability of the crystal structure of

the protein in complex with the antagonistic compounds risperidone and zotepine (19). This crystal structure has revealed insights regarding the 5-HT_{2A} recognition site, which can be divided into two regions: the orthosteric binding pocket, which is situated in a cleft formed by the transmembrane domains, and the extended binding site, which is responsible for ligand recognition. This extended binding site is anchored by a disulphide bridge between cysteine 148 (C148) in transmembrane domain 3 (TM-3) and cysteine C227 in extracellular loop 2 (ECL-2). Further studies support that another extracellular disulphide bridge between cysteines in extracellular loop 3 (ECL-3) could participate in stabilizing this extended binding site (20,21).

The TM-3 - ECL-2 disulphide bridge is conserved in more than 90 % of all GPCRs (22,23) and is involved in stabilising the extracellular region of the protein. It links TM-3, which is related to class A GPCR activation (24), and ECL-2, which acts as a lid over the orthosteric binding site (25,26). Therefore, it seems to be key for ligand binding selectivity (27), activation of different signalling pathways (28), and allosteric modulation (29,30). Molecular dynamics experiments have suggested that this bridge is established only in active GPCR conformations (31), further supporting its essentiality for GPCR activation.

In previous studies we have shown that the non-specific reduction of the extracellular domain of the 5-HT_{2A} receptor by dithiothreitol (DTT) leads to a decrease in [^{3}H]lysergic acid diethylamide ([^{3}H]LSD) specific binding and agonist efficacy, without affecting the homodimeric nature of the receptor. Modelling experiments suggest that the specific reduction of the TM-3 - ECL-2 disulphide bridge implies an increase in the flexibility of ECL-2, allowing it to be introduced into the orthosteric binding pocket and sterically prevent its interaction with ligands such as LSD (32). For these reasons, we hypothesised that C148 – C227 disulphide bridge may stabilize the orthosteric binding site of the homodimeric 5-HT_{2A} receptor, facilitating ligand binding. Thus, the aim of this work was to study its role on 5-

HT_{2A} receptor pharmacology, by using different constructs that are unable of maintaining this bridge.

2. Materials and methods

2.1.Chemical, plasmids and reagents

The *myc* N-terminally tagged and enhanced yellow fluorescent protein (eYFP) C-terminally tagged wild type 5-HT_{2A} receptor (WT) cloned in a pcDNA3.1 and previously used in our laboratory (33) was cloned into pcDNA5/FRT/TO, purchased from Invitrogen (Darmstadt, Hesse, Germany). Point mutations were introduced using QuickChange II XL Site Directed mutagenesis kit, purchased from Agilent Technologies (Cedar Creek, Texas, USA), following the instructions of the manufacturer (**Table 1**). Four plasmids were obtained: pcDNA5/FRT/TO *myc*-5-HT_{2A}-eYFP, pcDNA5/FRT/TO *myc*-5-HT_{2A}C148A-eYFP, pcDNA5/FRT/TO *myc*-5-HT_{2A}C227A-eYFP and pcDNA5/FRT/TO *myc*-5-HT_{2A}C148A/C227A-eYFP. Likewise, the same mutated constructs were introduced into a *Renilla* luciferase (Rluc) fusion protein expression vector (pRluc-N2), purchased from BioSignal Packard (Montreal, Quebec, Canada), containing the *myc*-5-HT_{2A} insert, to obtain pRluc-N2 *myc*-5-HT_{2A}C148A, pRluc-N2 *myc*-5-HT_{2A}C227A and pRluc-N2 *myc*-5-HT_{2A}C148A/C227A .

[^{3}H]LSD (specific activity: 82.9 Ci/mmol), [^{3}H]*myo*-inositol (specific activity: 20.3 Ci/mmol), RNA Binding YSi SPA Beads and OptiPhase Supermix scintillation cocktail were purchased from Perkin Elmer (Rodgau, Hesse, Germany). Universol™-ES liquid scintillation cocktail was purchased from MP Biomedical™ (Santa Ana, California, USA). Fura-2 QBT™ Calcium Kit was purchased from Molecular Devices (Sunnyvale, California, USA). Hanks Balanced Salt Solution (HBSS), HEPES, hygromycin B, paraformaldehyde, Hoechst 33342

dye, ER-tracker™ Red dye, Lipofectamine® LTX, coelenterazine h, zeocin, doxycycline and horseradish peroxidase (HRP) conjugated anti-glyceraldehyde-3-phosphate dehydrogenase (GAPDH) antibody, SDS-PAGE in Bolt™ 4 - 12% Bis-Tris Plus Gels and foetal bovine serum (FBS) were purchased from Thermo Fisher (Alcobendas, Madrid, Spain). The rabbit anti *myc*-tag antibody and the HRP-conjugated anti-rabbit antibody were purchased from Cell Signalling Technology (Danvers, Massachusetts, USA). Wheat germ agglutinin conjugated with Alexa Fluor 555 was purchased from Invitrogen (Paisley, Renfrewshire, UK). The goat anti-rabbit antibody conjugated with Alexa Fluor 647 was purchased from Abcam (Cambridge, Cambridgeshire, UK) Bovine serum albumin (BSA) Fraction V Fatty acid free was purchased from La Roche (Basel, Switzerland). The ECL™ Prime Western Blotting Detection Reagent was purchased from GE Healthcare (Little Chalfont, Buckinghamshire, UK). Radioimmunoprecipitation Lysis Buffer System (RIPA buffer) was purchased from Santa Cruz Biotechnology (Dallas, Texas, USA). All other chemicals and reagents were purchased from Sigma Aldrich (Taufkirchen, Bayern, Germany).

2.2.Stable cell line generation

Cell lines were generated using the Flp-In™ T-REx™ technology. Briefly, the Flp-In T-REx-293 cell line, derived from 293 human embryonic kidney (HEK293) cells and purchased from Invitrogen (Darmstadt, Hesse, Germany), resistant to zeocin, was co-transfected with the Flp-recombinase transfection vector pOG44 (purchased from Invitrogen; Darmstadt, Hesse, Germany) and pcDNA5/FRT/TO plasmids containing the human 5-HT_{2A} or its mutant constructs, using polyethyleneimine (PEI) in a 4:1 ratio. Twenty-four hours later, zeocin was removed from the medium and cells were selected for their acquired resistance to hygromycin B (200 µg/mL). The resulting colonies were expanded and cultured in

Dulbecco's modified Eagle's medium (DMEM) supplemented with 10 % (v/v) FBS, 200 µg/mL hygromycin B, 5 µg/mL blasticidin, 1 % (v/v) GlutaMAX™ and 1 % (v/v) penicillin/streptomycin (complete medium). Successful transfection of the plasmids and, therefore, presence of the receptor, was checked by seeding the transfectants (cell lines expressing WT, C148A, C227A, and C148A/C227A receptors) into clear-bottom 96-well plates (Perkin Elmer; Tres Cantos, Madrid, Spain), with medium supplemented with 10 ng/mL doxycycline. Twenty-four hours later, fluorescence microscopy images of eYFP-tagged receptorexpression were obtained using a High Content Imaging System (Operetta, Perkin Elmer). Only cells up to passage number 20 were used.

2.3.Binding assays in membrane fraction

Membrane fractions were prepared from the generated cell lines following a 24 hours receptor expression induction with 10 ng/mL doxycycline. Next, cells were harvested and pelleted by centrifugation at 800 ×*g* for 15 minutes at 4 ºC. Pelleted cells were then lysed in 50 mM Tris-HCl (pH 7.50) and homogenized with a Polytron homogenizer. The homogenate was centrifuged at 48000 ×*g* for 40 minutes at 4 ºC, and the resulting pellet was resuspended in 50 mM Tris-HCl (pH 7.50) at 4 ºC. Protein concentration was determined through the Bradford method using the Bio-Rad Protein Assay (Bio-Rad, California, USA) with BSA as the standard.

Binding experiments were carried out in clear flat-bottomed 96-well plates (Thermo Fisher; Alcobendas, Madrid, Spain). Here, eight different concentrations (0.08 nM to 10 nM) of [^{3}H]LSD were incubated with 60 µg protein/well in incubation buffer (50 mM Tris-HCl, pH 7.50). To study total binding (BT) of the different cell lines, each preparation was incubated with 1 nM of radioligand. Non-specific binding was determined by the addition of

1 μM methysergide. The reaction mixture was incubated at 37 °C for 30 min, after which 200 μl of each reaction mix were transferred to a Multiscreen GF/B 96-well filter plate (Millipore; Billerica, Massachusetts, USA), pretreated with 0.50 % (v/v) PEI, filtered, and washed six times with 250 μl wash buffer (50 mM Tris-HCl, pH 6.60), before the addition of 30 μl/well of Universol™. The radioactivity was measured in a Microbeta^2 2450 reader (Perkin Elmer).

2.4.Binding assays in whole cells

Whole cell binding experiments were carried out in Falcon® clear, flat-bottomed and tissue culture-treated 96-well plates (Corning; New York, USA) precoated with 20 μg/mL poly-D-lysine for 30 minutes at 22 ºC. Cells were seeded at an optimized density of 10^5 cells/well in complete medium supplemented with 10 ng/mL doxycycline. Twenty-four hours later, cells were incubated with 1 nM [^{3}H]LSD for 30 minutes at 37 ºC. In competition experiments, risperidone was added at different concentrations. Non-specific binding was determined by addition of 1 μM methysergide. Next, cells were washed three times with ice cold NaCl (0.90 % (v/v)) and lysed with absolute ethanol for 20 minutes at 4 ºC. Cell lysates were then transferred into a clear-bottom 96-well Flexiplate (Perkin Elmer, Tres Cantos, Madrid, Spain) and mixed with OptiPhase. Radioactivity was measured using a Microbeta^2 2450 reader (Perkin Elmer).

2.5.IPs accumulation measurements

Cells were seeded in Falcon® clear, flat-bottomed and tissue culture-treated 96-well plates precoated with 20 μg/mL poly-D-lysine for 30 minutes at 22 ºC, at an optimized density of $7.5 \cdot 10^4$ cells/well in complete medium. After 24 hours, the medium was replaced

by DMEM containing 10 μCi/mL of [^{3}H]*myo*-inositol and 10 ng/mL doxycycline. Twenty-four hours later, cells were washed with HBSS supplemented with 20 mM HEPES, 20 mM LiCl, and 2 % (w/v) BSA (pH 7.55) for 10 minutes, and then incubated 20 minutes with the indicated compounds. Next, cells were lysed with 100 mM of formic acid for 30 minutes, and an aliquot of 20 μL was mixed in a clear-bottom 96-well Flexiplate with a 1/16 dilution of RNA YSi binding SPA beads. Radioactivity was measured in a Microbeta^2 2450 reader (Perkin Elmer).

2.6.Calcium mobilization measurements

Cells were seeded into clear, flat-bottomed, black-walled, 384-well plates (Greiner Bio-One, Frickenhausen, Baden-Württemberg, Germany) precoated with 20 μg/mL poly-D-lysine for 30 minutes at 22 ºC. Cell density was optimized to $6 \cdot 10^4$ cells/well in 25 μL of complete medium supplemented with 10 ng/mL doxycycline. After 24 hours, dye loading buffer was prepared by dissolving the contents of one vial of dye (Fura-2 QBT™ Calcium Kit) with a volume of 10 mL HBSS, supplemented with 20 mM HEPES and 5 mM probenecid and adjusted to pH 7.40. Then, 25 μL of dye loading buffer was added to each well and incubated for 1 hour at 37 °C. Changes in fluorescence due to intracellular calcium mobilization ($\lambda_{ex(1)}$ 340 nm, $\lambda_{ex(2)}$ 380 nm, λ_{em} 540 nm) were measured using a calcium imaging plate reader system (FDSS7000EX, Hamamatsu®) every second after establishing the base line. The calcium peak in response to agonists occurred from 10 s to 20 s following stimulation. Antagonist compounds were preincubated with the cells 3 minutes before addition of the agonist. Output was calculated as the ratio between 340 nm and 380 nm wavelength signals at each time point during the assay. From the ratiometric signal trace, the maximum-minimum value was calculated.

2.7.Fluorescence microscopy

In order to detecting the receptor expression in cell compartments, two different approaches were employed: eYFP fluorescence intensity detection and immunocytochemistry techniques.

For eYFP fluorescence intensity measurements, cells were seeded in clear-bottom 96-well plates (PerkinElmer; Tres Cantos, Madrid, Spain) precoated with 20 µg/mL poly-D-lysine for 30 minutes at 22 ºC at an optimized density of $4 \cdot 10^4$ cells/well and in the presence of 10 ng/mL doxycycline. Twenty-four hours later, cells were fixed with 4 % (w/v) paraformaldehyde for 10 minutes at 22 ºC, washed, and incubated with 1 µM ER-tracker™ Red for 1 hour and with 2.50 µg/mL Hoechst 33342 for 30 minutes at 22 ºC. After washing with HBSS twice, cells were imaged using the High Content Imaging System Operetta (Perkin Elmer) under the brightfield channel and three fluorescent channels: λ_{ex} 500 nm and λ_{em} 540 nm to measure YFP fluorescence; λ_{ex} 570 nm and λ_{em} 615 nm to measure ER-tracker™ Red fluorescence, and λ_{ex} 350 nm and λ_{em} 445 nm, to measure Hoechst 33342 fluorescence. Image Analysis was conducted with the Harmony High Content Imaging and Analysis Software (Perkin Elmer), to quantify: total receptor expression, by measuring fluorescence intensity of YFP in whole cells; receptor presence in the cell membrane, by measuring fluorescence intensity of YFP in the plasmatic membrane; and receptor presence in the endoplasmic reticulum (ER), by measuring co-localization of the YFP receptor and the stained ER.

In the immunocytochemistry approach, cells were seeded in clear-bottom 96-well plates (PerkinElmer; Tres Cantos, Madrid, Spain) precoated with 20 µg/mL poly-D-lysine for 30 minutes at 22 ºC at an optimized density of $5 \cdot 10^4$ cells/well. In half of the wells, receptor

expression was induced by exposition to 10 ng/mL doxycycline. Twenty-four hours later, cells were fixed with 4 % (w/v) paraformaldehyde for 10 minutes at 22 ºC, washed and incubated with 2.50 µg/mL Hoechst 33342 and 1.50 µg/mL wheat germ agglutinin conjugated with Alexa Fluor 555 (W32464; Invitrogen, Paisley, UK) in HBSS (pH 7.40). After 30 minutes at 37ºC, cells were treated with a blocking buffer containing 5 % BSA in HBSS at 22 ºC for 30 minutes. Then, cells were exposed to a 1:400 solution of an anti-*myc*-tag rabbit antibody in DMEM at 4 ºC. Eighteen hours later, cells were washed and incubated for one hour with a 1:200 solution of a goat anti-rabbit antibody conjugated with Alexa Fluor 647. After washing with HBSS twice, cells were imaged using the High Content Imaging System Operetta (Perkin Elmer) under the brightfield channel and three fluorescent channels: λex 650 nm and λem 670 nm to measure Alexa Fluor 647 (which stained the receptor); λex 550 nm and λem 580 nm to measure Alexa Fluor 555 (which stained the plasmatic membrane), and λex 350 nm and λem 445 nm, to measure Hoechst 33342. Image Analysis was conducted with the Harmony High Content Imaging and Analysis Software (Perkin Elmer) to quantify receptor presence in the cell membrane, by measuring Alexa Fluor 647 intensity only in the plasmatic membrane, stained with Alexa Fluor 555. Fluorescence intensity in cells non exposed to doxycycline was subtracted from fluorescence intensity in cells exposed to doxycycline.

2.8.Bioluminescence Resonance Energy Transfer (BRET)

BRET saturation experiments were performed in transiently transfected HEK293T/17, cultured in DMEM supplemented with 10 % (v/v) FBS, 1 % (v/v) GlutaMAX™ and 1 % (v/v) penicillin/streptomycin. Cells were seeded at a density of $5 \cdot 10^4$ cells/well in white, flat-bottomed 96-well plates (Greiner Bio-One, Frickenhausen, Baden-Württemberg, Germany). Then, cells were co-transfected with a fixated amount of pRluc-N2-GPCR plasmid (1.25 ng/well) and increasing amounts of pcDNA3-GPCR-YFP plasmid (up to 100 ng/well, unless

otherwise noted) using Lipofectamine® LTX in a 2.50:1 ratio. DNA amount was completed up to 150 ng DNA/well with empty pcDNA3. Twenty-four hours later, YFP expression (YFP_c) was quantified in each well by direct measurement of the fluorescence emission at λ_{em} 530 nm, after excitation at λ_{ex} 480 nm in an Infinite® M1000 microplate reader (Tecan, Männedorf, Switzerland). Then, the cells were incubated with 125 µM coelenterazine h for 10 minutes at 37 ºC, and BRET was quantified by dual bioluminescence measurement (370 – 480 nm filter for Rluc emission and 520 – 570 nm filter for YFP emission). Ten minutes later, total luminescence (400 – 700 nm filter) was quantified as a measure of donor expression ($Rluc_q$). Results were expressed as mili net BRET units, which correspond to the net BRET ratio values multiplied by 1000 and were represented as a function of the acceptor expression/donor expression ($YFP_c/Rluc_q$).

2.9.Western blotting

Cells were grown for 24 hours in the presence of 10 ng/mL doxycycline and lysed in RIPA buffer supplemented with 1 % (v/v) sodium orthovanadate, 1 % (v/v) phenylmethylsulphonyl fluoride, and 1 % (v/v) protease inhibition cocktail, for 1 hour at 4 ºC. The suspension was centrifuged at 14000 ×*g* for 30 minutes and the supernatant was collected for protein concentration quantification by Bradford Assay. Equivalent amounts of protein (60 µg) were incubated at 37 ºC for 20 minutes in 4× lithium dodecyl sulphate loading buffer, resolved by SDS-PAGE in Bolt™ 4 - 12% Bis-Tris Plus Gels and transferred to a polyvinylidene difluoride membrane. The blot was blocked with 5 % (w/v) BSA for 1 hour at 22 ºC and incubated overnight with the anti-*myc* tag rabbit primary antibody (1:1000) at 4 ºC. After extensive washing (1 M Tris-HCl; 1.15 M NaCl; 0.10 % (v/v) Tween 20; pH 7.70), the blot was incubated with an anti-rabbit HRP-conjugated antibody (1:5000) for 1 hour at 22 ºC.

Detections were performed by enhanced chemiluminescence using the ECL™ Prime Western Blotting Detection Reagent. To quantify the loading control, GAPDH, blots were incubated with an HRP-conjugated anti-GAPDH antibody (1:10000) overnight at 4 ºC and resolved.

2.10. Data analysis

Saturation curves were fitted to a hyperbolic function in GraphPad Prism 5.0 (GraphPad Software, La Jolla, USA). The percentage of specific binding (SB) was calculated for each cell line as ((BT-NSB)/BT)·100; where BT is the total binding of the radioligand and NSB is the non-specific binding of the radioligand. Concentration-response curves were analysed through non-linear fitting using GraphPad Prism 5.0 software by applying both a four-parameter logistic equation and a five-parameter logistic equation, and statistical comparisons between fits were performed with extra sum-of-squares F Test, being the statistical significance set at $P < 0.05$. In BRET saturation experiments, BRET efficiency was a function of YFP emission and Rluc emission, as previously described (32). Statistical comparisons between different parameters were carried out by one-way ANOVA followed by Tukey's multiple comparisons test, and statistical significance was set at $P < 0.05$.

3. Results

3.1. The C148 – C227 disulphide bridge is critical for ligand binding to 5-HT_{2A} receptor

In order to assess whether the C148 – C227 disulphide bridge is related to 5-HT_{2A} receptor ligand binding, we substituted the cysteine residues involved in this bridge to alanines, to form single and double mutated receptors. They were stably expressed in

HEK293 cells using Flp-In™ T-REx™ technology, to generate four isogenic cell lines with doxycycline-inducible receptor expression (34): WT, C148A, C227A and C148A/C227A cell lines.

To evaluate the effect of the C148 and C227 to alanine substitutions on ligand binding, we used [^{3}H]LSD as a radioligand in the membrane fraction of the receptor expressing cells. Despite the specific binding of the WT receptor to [^{3}H]LSD (B_{max} = 513.30 ± 7.69 fmol/mg of protein and K_D = 0.78 ± 0.08 nM, **Figure 1A**), we found that the specific binding obtained for the C148A, C227A, and C148A/C227A mutated receptors was blunted when compared to WT, and similar to that obtained for the non-transfected (NT) cell line (**Figure 1B**).

To study the effect of absence of the C148 – C227 disulphide bridge in ligand binding in whole cells, we used [^{3}H]LSD as a radioligand and found the affinity of risperidone in the WT cell line to be 0.21 nM (**Figure 2A**), which is similar to the affinity reported in the literature (35). The specific binding of [^{3}H]LSD was higher in the WT cells than in the NT cells. The mutated receptors showed a specific binding to [^{3}H]LSD that was 50 % lower than the specific binding of the WT receptor. Besides, the specific binding obtained in the mutated receptors was higher than the specific binding obtained in NT cells (**Figure 2B**).

3.2. Signalling via PLC is impaired when the C148 – C227 disulphide bridge is broken

Given the modest specific binding of [^{3}H]LSD observed in whole cells expressing the mutated receptors, we studied the effect of substituting C148 and C227 to alanines on the intracellular signalling pathways by measuring PLC activation at two levels: IPs accumulation and calcium mobilization.

We validated the cell line expressing the WT receptor with the endogenous agonist serotonin (5-HT) and the hallucinogens (±)2,5-dimethoxy-4-iodoamphetamine ((±)DOI) and LSD, by measuring IPs accumulation (**Figure 3A**). Both (±)DOI and LSD behaved as partial agonists with similar potencies to those previously reported (36). However, the potency obtained for 5-HT was higher than the previously described (37) (**Table 2**). The effect of clozapine and haloperidol was evaluated by inhibition of the effect exerted by (±)DOI at its EC_{80} (0.10 μM). The antagonist potency (K_B) was 37.60 nM for clozapine and 685 nM for haloperidol (**Figure 3B** and **3C**, respectively).

Next, we studied the effect of the mutations on IPs accumulation elicited by the three agonists. We observed that IPs signalling was dampened in C148A, C227A, and C148A/C227A cell lines (**Figure 3D**).

To assess whether the C148 – C227 disulphide bridge is necessary to activate PLC, we proposed the study of its activation at a different level, by measuring calcium mobilization (**Figure 4A**). The potencies and efficacies elicited by the agonists 5-HT, (±)DOI, and LSD in the WT cell line were in agreement with those reported in literature (38) (**Table 3**). When evaluating the inhibition of the effect exerted by (±)DOI at its EC_{80} (0.10 μM) by the two antagonists clozapine and haloperidol, the potencies obtained were 4.98 nM and 92.60 nM, respectively (**Figure 4B** and **4C**).

Then, we studied the effect of the mutations in the calcium mobilization response elicited by the three agonists. We found that this response was impaired in C148A, C227A, and C148A/C227A cell lines (**Figure 4D**), even when using saturating concentrations of agonists 5-HT and (±)DOI (**Figure 4E**). It was not possible measuring the response to 100 μM LSD owing to its insolubility in aqueous medium

3.3.The absence of the C148 – C227 disulphide bridge in the 5-HT_{2A} receptor conditions its trafficking to the cell membrane

Cell surface expression of the receptor in each generated cell line was evaluated by the induction of the receptor expression through treatment with 10 ng/mL doxycycline for 24 h (**Figure 5**, green). Then, we stained cell nuclei with Hoechst dye (**Figure 5**, blue) and endoplasmic reticulum with ER-tracker™ red dye (**Figure 5**, red).

We then measured total fluorescence intensity of YFP (I_T) in the cells and considered the WT cell line expression as 100 %. C148A mutated receptor expression was higher than WT, while C227A receptor expression was lower (**Figure 6**). In addition, when measuring the localization of the receptor on the cell surface, the mutations induced a decrease in receptor trafficking to the cell membrane by up to 50 %, compared to WT (**Figure 7A**). Besides, receptor expression of C148A and C148A/C227A receptor mutants in the cell membrane was higher than C227A receptor. This was confirmed with immunocytochemistry experiments, (**Figure 7B**).

The decrease of the receptor presence in the cell membrane might be explained by a higher retention of the aberrant receptor in the endoplasmic reticulum. To study it, we measured fluorescence intensity of YFP in the endoplasmic reticulum (I_{RE}), compared to the fluorescence intensity of YFP in the whole cell. None of the mutations resulted in a higher retention of the receptor in the endoplasmic reticulum (**Figure 8**).

3.4.The dimeric nature of the 5-HT_{2A} receptor is retained in the absence of the C148 – C227 disulphide bridge

To assess the role of the C148 – C227 disulphide bridge in receptor oligomerization, we carried out saturation BRET experiments, where the receptor linked to the Rluc donor was fixed, and the same receptor linked to the eYFP acceptor was titrated to construct hyperbolic curves (**Figure 9A**). The $BRET_{50}$ obtained for the WT - WT pair was 31.79, similar to that obtained for the C227A – C227A single mutant pair ($BRET_{50}$ = 25.08), and for the C148A/C227A – C148A/C227A double mutant pair ($BRET_{50}$ = 40.24). However, the C148A – C148A single mutant pair resulted in a higher $BRET_{50}$ ($BRET_{50}$ = 81.90, $P < 0.01$).

The $BRET_{max}$ obtained for WT and the mutated receptor was similar, independently of the amount of transfected DNA (**Figure 9B**). Increasing the total amount of transfected DNA per well (from 100 ng per well to 150 ng per well) did not change the $BRET_{max}$, although it did increase receptor expression, measured as $YFP_c/Rluc_q$ ratio (**Figure 9C**) in the WT receptor and in the C227A receptor. Moreover, the C227A – C227A single mutant pair and the C148A/C227A – C148A/C227A double mutant pair showed lower receptor expression than the WT - WT and the C148A - C148A single mutant pairs.

To assess homodimerization of the 5-HT_{2A} receptor in the absence of the C148 – C227 disulphide bridge, we used the cell lysates of the WT cell line and the C148A, C227A and C148A/C227A cell lines for western blotting. As a negative control, the lysate of NT cells was used. We found that the homodimeric form of the receptor was retained in all mutant cell lines (**Figure 10A**), as well as the relation dimer to monomer (**Figure 10B)**.

4. Discussion

The major finding of this study was that in the homodimeric 5-HT_{2A} receptor, the C148 – C227 disulphide bridge is key for ligand recognition. Although approximately 50 % of the mutated receptors reach the cell membrane, their affinity and potency for selected ligands

appear to be reduced. This suggests that the TM-3 and ECL-2 link in 5-HT_{2A} receptor is crucial to properly accommodate ligands.

Like most GPCRs, the human 5-HT_{2A} receptor anchors TM-3 and ECL-2 by an extracellular disulphide bridge formed between $C148^{3.25}$ and $C227^{ECL\text{-}2}$. Apart from this bond, in GPCRs, extracellular cysteines can form more disulphide bridges, which are usually involved in the stabilization of different conformations of the receptor, and, hence, in ligand recognition.

According to extracellular disulphide bridges, the relevance of their formation in GPCR pharmacology depends on the studied receptor. Therefore, GPCRs can be classified into six groups: one that only contains the TM-3 - ECL-2 linkage, one in which the N-terminal domain is connected to ECL-2, one in which the N-terminal domain is connected to ECL-3, and the last three with different patterns of intra-helix disulphide bridges (39). The recent co-crystallisation of 5-HT_{2A} receptor in the presence of risperidone and zotepine revealed that $C148^{3.25}$ and $C227^{ECL\text{-}2}$ are involved in the formation of an extracellular disulphide bridge (19). Moreover, the presence of another extracellular disulphide bridge between two cysteines in ECL-3 is energetically favourable (20,21).

In the human 5-HT_{2A} receptor, extracellular disulphide bridges have been reported to play an important role in ligand recognition. Iglesias *et al*. demonstrated that the non-specific reduction of the extracellular domains of 5-HT_{2A} receptor with DTT led to a decrease in ligand binding and ability of activating different intracellular signalling pathways by different ligands, without affecting the homodimeric nature of 5-HT_{2A} receptor. Molecular dynamics experiments have shown that breaking the TM-3 - ECL-2 disulphide bridge results in a collapse of the orthosteric binding site, because of the freedom that ECL-2 adopts (32).

To specifically evaluate the effect of the C148 – C227 disulphide bridge in ligand recognition by the 5-HT_{2A} homodimeric receptor, we generated three constructs that cannot stablish this disulphide bridge. We achieved this by mutating the cysteines involved in the TM-3 - ECL-2 disulphide bridge into alanines: the two single mutant constructs, C148A and C227A, leave a free cysteine, whereas the double mutant, C148A/C227A, does not. With these constructs, we generated four stable cell lines that express the WT or the mutated receptor (C148A, C227A, or C148A/C227A) employing Flp-In™ T-REx™ technology, for studying binding properties, PLC activation, receptor trafficking and homodimerization of the 5-HT_{2A} receptor in the absence of the C148 – C227 disulphide bridge. We decided to employ an inducible receptor expression system because the non-induced cells emerged as self-control of receptor expression, as well as it allows fine-tuning receptor expression, avoiding the 5-HT_{2A} receptor internalization (40,41) that would led to misleading results. Cell line generation was checked by microscopy techniques, were we probed that all the constructs were expressed in each cell line.

In order to study the influence of this disulphide bridge on 5-HT_{2A} receptor binding, we compared the specific binding of [^{3}H]LSD of the mutated receptors to the WT receptor in the cell membrane fraction. We found that the absence of this disulphide bond stunted 5-HT_{2A} binding ability, decreasing the specific binding up to the NT cell line levels. That suggests that the C148 – C227 disulphide bridge is crucial for ligand binding in 5-HT_{2A} receptor, as observed for the corresponding conserved disulphide bond in the adenosine A_1 receptor (42), or in the adrenergic α_{1B} receptor (43).

Binding experiments carried out in membrane fractions provide good signal to noise ratios whereas whole cell binding experiments allow the study of radioligand binding in living cells and their intracellular compartments (44). To assess ligand binding in the mutated receptors, we evaluated specific binding of [^{3}H]LSD in whole cells. Although there was a

decrease in the specific binding of [^{3}H]LSD in the three mutant constructs compared to WT, it was higher than the specific binding obtained in the NT cells. Unlike membrane fraction binding, [^{3}H]LSD binds to a small amount of mutated receptor population in living cells. These differences could be related to the cell environment that living cells is providing to the receptors, maintaining more favourable conformations to bind ligands, apart from the fact that membrane fraction imply purification of the receptor whereas in living cells the whole pool of receptor is available to bind ligands. Therefore, we investigated the possibility of amplifying the binding measurements by studying PLC activation by the agonists 5-HT, (±)DOI, and LSD using two different approaches: measuring IPs accumulation, which is a direct consequence of activating PLC, and measuring calcium mobilization, as a result from IPs accumulation.

Subsequently, we found that none of the cell lines expressing the mutated receptor was able to increase neither the IPs accumulation, nor the calcium mobilization upon different agonist treatments. This is in agreement with the proposal that breaking the C148 – C227 disulphide bridge results in the collapse of the orthosteric binding pocket (32), unless the receptor was so aberrant that it would not be properly trafficked to the cell membrane.

It has been reported that some GPCRs can be retained in the endoplasmic reticulum or be degraded inside the cell due to amino acid substitutions. For example, the double mutation, $C^{N\text{-terminal}}A/C^{7.25}A$, in the platelet receptor P2Y12 or $C^{ECL\text{-}2}A/C^{ECL\text{-}2}A$ in the adrenergic β_1 prevent receptor trafficking to the cell membrane (31). The $C^{3.25}A$ and $C^{ECL\text{-}2}A$ mutations impede receptor trafficking in the adenosine A_1 receptor (42), or reduced trafficking by up to 13 % in GPR39 (39), up to 17 % in chemokine CCR1 receptor, or up to 52 % in chemokine CCR5 receptor (45). However, the same substitutions in adenosine A_2 (A_2) receptor did not compromise receptor trafficking to cell membrane (42).

To study if the substitutions compromise 5-HT_{2A} receptor trafficking to the cell membrane, we took advantage of the eYFP tag, and we stained the nuclei and the endoplasmic reticulum. Prior to study receptor localisation in the cell, we measured receptor expression in whole cells. C148A/C227A mutated receptor expression in the whole cells was similar to that obtained with the WT receptor, but C148A receptor expression was higher, and the C227A receptor expression was lower. Due to the fact that the Flp-In™ technology allows the generation of isogenic cell lines (34), the observed differences must be related to the nature of the generated receptors, so receptor trafficking to the cell membrane would be compromised as well

Once we measured receptor localisation within the cell membrane, we observed that just around 50 % of the mutated receptors reached the cell membrane when compared to WT, as it happens in adenosine A_2 receptor, where the substitution of extracellular cysteines by alanines reduced up to 40 % the receptor trafficking to the cell membrane (46). Besides, C227A receptor localisation within the cell membrane was lower than the C148A and the C148A/C227A receptors. We confirmed this expression pattern by an immunocytochemistry approach, emphasizing that the differences observed are related to the nature of the receptor: while the C148A/C227A receptor is unable to stablish any disulphide bridges, the single mutants leave a free cysteine to react with other extracellular cysteines, to compensate the absence of the C148 – C227 disulphide bridge (**Figure 11**). If that happens, the conformation of the receptor would be different to the native form, and hence, detected as aberrant.

Receptors that did not localise within the cell membrane could be retained in the endoplasmic reticulum, the first checkpoint of correct protein folding in the cell. A single mutation in a critical amino acid residue may have resulted in total retention of the protein in the endoplasmic reticulum, as is the case with the follicle-stimulating hormone receptor (47). In the 5-HT_{2A} receptor, mutating the cysteines involved in the C148 – C227 disulphide bridge

may have increased endoplasmic reticulum retention due to stabilisation of wrong receptor conformations. Then, we measured localisation of the native and mutated receptors in the endoplasmic reticulum. We found no difference between the mutated and the WT receptors, suggesting that the substitutions do not increase the localisation of the 5-HT_{2A} receptor in the endoplasmic reticulum, as is the case in the adenosine A_{2A} receptor (48). Thus, the decrease in the membrane localisation of the mutated receptor is likely due to the presence of the receptor in other intracellular compartments, such as lysosomes or endosomes, which might led to receptor degradation.

An extensive degradation could be related to impaired dimer formation. Previously published data has proposed that the GPCRs that exist as dimers migrate to the cell membrane as complexes (49). Therefore, the dimeric state of the receptor may condition receptor trafficking. Specifically, the TM-3 - ECL-2 disulphide bridge participates in muscarinic M_3 receptor homodimerization (50). In the 5-HT_{2A} receptor, the non-specific reduction of extracellular disulphide bridges with DTT did not alter its homodimeric state (32) but this treatment is limited to the receptor that actually reaches the cell membrane. To understand if the C148A, C227A, and C148A/C227A substitutions could condition the homodimerization of 5-HT_{2A} receptor, we carried out BRET and western blot studies.

BRET studies demonstrated that all mutated 5-HT_{2A} receptors retained their ability to oligomerize. These studies also revealed that the C148A protomers had less avidity for each other because the $BRET_{50}$ values for the C148A mutant were higher than the WT receptor. The C148A single mutant left a cysteine in the ECL-2 which was free to move and interact with other extracellular cysteines. The ECL-2 domain is thought to play a key role in the dimeric interface of the adenosine A_1 receptor (51), therefore, altering the structure of this domain may result in changes in the dimeric nature of this receptor. Although the ECL-2 has not been reported to participate in the 5-HT_{2A} homodimeric interface (52), these results imply

that the conformation adopted by the C148A substituted receptor is less favourable for dimerization, probably because of the additional freedom adopted by the ECL-2.

BRET studies also showed that the C227A and C148A/C227A receptor expression, which is defined by the emission ratio $YFP_c/Rluc_q$, was lower than the WT receptor. Increasing the amount of transfected DNA per well resulted in an increase in the receptor expression in all the constructs, but again, expression of C227A and C148A/C227A was lower compared to the WT receptor. Taken together with microscopy data, this suggests that the cysteine in the ECL-2 is crucial for receptor expression.

We confirmed that the C148 – C227 disulphide bridge does not participate in 5-HT_{2A} oligomerization meaning that the stunted membrane trafficking is not due to changes in receptor complexing. To confirm 5-HT_{2A} receptor homodimerization in the presence of the mutations, we carried out western blot experiments with whole cell lysates, taking advantage of the *myc*-tag. We corroborated that the 5-HT_{2A} receptor homodimerizes, as there were two immunoreactive bands; a 75 kDa band, the monomer; and a 150 kDa band, the homodimer, in the WT cell line as well as in the C148A, C227A, and C148A/C227A cell lines, as well as no differences in the dimer to monomer ratio were observed. The C148 – C227 disulphide bridge does not participate in the homodimeric interface of the 5-HT_{2A} receptor.

In summary, we demonstrated that the C148 – C227 disulphide bridge of the homodimeric 5-HT_{2A} receptor is essential for its ligand recognition and trafficking to the cell membrane. Moreover, ECL-2 emerged as a key factor in maintaining proper receptor conformation. Although there is evidence that another extracellular disulphide bridge might be stablished in 5-HT_{2A} receptor, we show here that the C148 – C227 disulphide bridge is crucial to 5-HT_{2A} receptor pharmacology. The insights gained from this work may aid the design of novel antipsychotic drugs that target the 5-HT_{2A} receptor.

Acknowledgements

This work was supported by the Spanish Ministry of Economy and Competitiveness (SAF2014-57138-C2-1-R and SAF2017-85225-C3-1-R) and the European Regional Development Fund (ERDF). MC and LGG were supported by a grant from the *Consellería de Cultura, Educación y Ordenación Universitaria*, partially co-funded by the European Social Fund (ESF) program.

Conflict of interest

No conflict of interest

References

1. Masson J, Emerit MB, Hamon M, Darmon M. Serotonergic signaling: Multiple effectors and pleiotropic effects. Wiley Interdiscip Rev Membr Transp Signal. 2012;1(6):685–713.

2. Meltzer HY. What's atypical about atypical antipsychotic drugs? Curr Opin Pharmacol. 2004;4(1):53–7.

3. Yadav PN, Kroeze WK, Farrell MS, Roth BL. Antagonist Functional Selectivity : 5-HT 2A Serotonin Receptor Antagonists Differentially Regulate 5-HT 2A Receptor Protein Level In Vivo. Pharmacology. 2011;339(1):99–105.

4. Berg KA, Maayani S, Goldfarb J, Scaramellini C, Leff P, Clarke WP. Effector

pathway-dependent relative efficacy at serotonin type 2A and 2C receptors: evidence for agonist-directed trafficking of receptor stimulus. Mol Pharmacol. 1998;54(1):94–104.

5. Marti-Solano M, Iglesias A, de Fabritiis G, Sanz F, Brea J, Loza MI, et al. Detection of New Biased Agonists for the Serotonin 5-HT2A Receptor: Modeling and Experimental Validation. Mol Pharmacol. 2015;87(4):740–6.

6. Iglesias A, Cimadevila M, Cadavid MI, Loza MI, Brea J. Serotonin-2A homodimers are needed for signalling via both phospholipase A2and phospholipase C in transfected CHO cells. Eur J Pharmacol. 2017;800:63–9.

7. Teitler M, Klein MT. A new approach for studying GPCR dimers: drug-induced inactivation and reactivation to reveal GPCR dimer function in vitro, in primary culture, and in vivo. Pharmacol Ther. 2012;133(2):205–17.

8. Albizu L, Holloway T, González-Maeso J, Sealfon SC. Functional crosstalk and heteromerization of serotonin 5-HT2A and dopamine D2 receptors. Neuropharmacology. 2011;61(4):770–7.

9. Viñals X, Moreno E, Lanfumey L, Cordomí A, Pastor A, de La Torre R, et al. Cognitive Impairment Induced by Delta9-tetrahydrocannabinol Occurs through Heteromers between Cannabinoid CB1 and Serotonin 5-HT2A Receptors. PLoS Biol. 2015;13(7):e1002194.

10. Borroto-Escuela DO, Li X, Tarakanov AO, Savelli D, Narváez M, Shumilov K, et al. Existence of Brain 5-HT1A–5-HT2A Isoreceptor Complexes with Antagonistic Allosteric Receptor–Receptor Interactions Regulating 5-HT1A Receptor Recognition. ACS Omega. 2017;2(8):4779–89.

11. González-Maeso J, Ang RL, Yuen T, Chan P, Weisstaub N V, López-Giménez JF, et al. Identification of a serotonin/glutamate receptor complex implicated in psychosis. Nature. 2008;452(7183):93–7.

12. Moreno JL, Muguruza C, Umali A, Mortillo S, Holloway T, Pilar-Cuellar F, et al. Identification of three residues essential for 5-hydroxytryptamine 2A-metabotropic glutamate 2 (5-HT2A-mGlu2) receptor heteromerization and its psychoactive behavioral function. J Biol Chem. 2012;287(53):44301–19.

13. Moreno JL, Miranda-Azpiazu P, García-Bea A, Younkin J, Cui M, Kozlenkov A, et al. Allosteric signaling through an mGlu2 and 5-HT2A heteromeric receptor complex and its potential contribution to schizophrenia. Sci Signal. 2016;9(410):ra5.

14. Fuxe K, Marcellino D, Woods AS, Giuseppina L, Antonelli T, Ferraro L, et al. Integrated signaling in heterodimers and receptor mosaics of different types of GPCRs of the forebrain: Relevance for schizophrenia. J Neural Transm. 2009;116(8):923–39.

15. Pei L, Li S, Wang M, Diwan M, Anisman H, Fletcher PJ, et al. Uncoupling the dopamine D1-D2 receptor complex exerts antidepressant-like effects. Nat Med. 2010;16(12):1393–5.

16. Pellissier LP, Barthet G, Gaven F, Cassier E, Trinquet E, Pin JP, et al. G protein activation by serotonin type 4 receptor dimers: Evidence that turning on two protomers is more efficient. J Biol Chem. 2011;286(12):9985–97.

17. Corriden R, Kilpatrick LE, Kellam B, Briddon SJ, Hill SJ. Kinetic analysis of antagonist-occupied adenosine-A3 receptors within membrane microdomains of individual cells provides evidence of receptor dimerization and allosterism. FASEB J. 2014;28(10):4211–22.

18. Springael JY, Minh PN Le, Urizar E, Costagliola S, Vassart G, Parmentier M. Allosteric modulation of binding properties between units of chemokine receptor homo- and hetero-oligomers. Mol Pharmacol. 2006;69(5):1652–61.

19. Kimura KT, Asada H, Inoue A, Kadji FMN, Im D, Mori C, et al. Structures of the 5-HT2A receptor in complex with the antipsychotics risperidone and zotepine. Nat Struct Mol Biol. 2019;26(2):121–8.

20. Bateman A. UniProt: A worldwide hub of protein knowledge. Nucleic Acids Res. 2019;47(D1):D506–15.

21. Mozumder S, Bej A, Srinivasan K, Mukherjee S, Sengupta J. Comprehensive structural modeling and preparation of human 5- HT 2A G- protein coupled receptor in functionally active form. Biopolymers. 2019;e23329.

22. Venkatakrishnan A, Deupi X, Lebon G, Tate CG, Schertler GF, Babu MM. Molecular signatures of G-protein-coupled receptors. Nature. 2013;494(7436):185–94.

23. Wheatley M, Wootten D, Conner MT, Simms J, Kendrick R, Logan RT, et al. Lifting the lid on GPCRs: The role of extracellular loops. Br J Pharmacol. 2012;165(6):1688–703.

24. Shan J, Khelashvili G, Mondal S, Mehler EL, Weinstein H. Ligand-dependent conformations and dynamics of the serotonin 5-HT(2A) receptor determine its activation and membrane-driven oligomerization properties. PLoS Comput Biol. 2012;8(4):e1002473.

25. Wacker D, Wang S, Mccorvy JD, Shoichet BK, Dror RO, Correspondence BLR, et al. Crystal Structure of an LSD-Bound Human Serotonin Receptor. Cell. 2017;168:377–89.

26. Nguyen ATN, Baltos J-A, Thomas T, Nguyen TD, Muñoz LL, Gregory KJ, et al. Extracellular Loop 2 of the Adenosine A1 Receptor Has a Key Role in Orthosteric Ligand Affinity and Agonist Efficacy. Mol Pharmacol. 2016;90(6):703–14.

27. De Filippo E, Hinz S, Pellizzari V, Deganutti G, El-Tayeb A, Navarro G, et al. A2A and A2B adenosine receptors: the extracellular loop 2 determines high (A2A) or low affinity (A2B) for adenosine. Biochem Pharmacol. 2019;113718.

28. Wootten D, Reynolds CA, Smith KJ, Mobarec JC, Koole C, Savage EE, et al. The extracellular surface of the GLP-1 receptor is a molecular trigger for biased agonism. Cell. 2016;165(7):1632–43.

29. Soave M, Cseke G, Hutchings CJ, Brown AJH, Woolard J, Hill SJ. A monoclonal antibody raised against a thermo-stabilised β 1 -adrenoceptor interacts with extracellular loop 2 and acts as a negative allosteric modulator of a sub-set of β 1 -adrenoceptors expressed in stable cell lines. Biochem Pharmacol. 2018;147:38–54.

30. Nguyen ATN, Vecchio EA, Thomas T, Nguyen TD, Aurelio L, Scammells PJ, et al. Role of the second extracellular loop of the adenosine A1 receptor on allosteric modulator binding, signaling, and cooperativity. Mol Pharmacol. 2016;90(6):715–25.

31. Zhang Q, Zhou M, Zhao L, Jiang H, Yang H. Dynamic States of the Ligand-Free Class A G Protein-Coupled Receptor Extracellular Side. Biochemistry. 2018;57(32):4767–75.

32. Iglesias A, Cimadevila M, la Fuente RA de, Martí-Solano M, Cadavid MI, Castro M, et al. Serotonin 2A receptor disulfide bridge integrity is crucial for ligand binding to different signalling states but not for its homodimerization. Eur J Pharmacol. 2017;815:138–46.

33. Brea J, Castro M, Giraldo J, López-Giménez JF, Padín JF, Quintián F, et al. Evidence for Distinct Antagonist-Revealed Functional States of 5HT2A Homodimers. Mol Pharmacol. 2009;75(6):1380–91.

34. Ward RJ, Alvarez-Curto E, Milligan G. Using the Flp-In™ T-Rex™ System to Regulate GPCR Expression. In: Methods in molecular biology (Clifton, NJ). 2011. p. 21–37.

35. Kroeze WK, Hufeisen SJ, Popadak BA, Renock SM, Steinberg S, Ernsberger P, et al. H1-histamine receptor affinity predicts short-term weight gain for typical and atypical antipsychotic drugs. Neuropsychopharmacology. 2003;28(3):519–26.

36. Lopez-Gimenez JF, Villazon M, Brea J, Loza MI, Palacios JM, Mengod G, et al. Multiple Conformations of Native and Recombinant Human 5-Hydroxytryptamine2A Receptors Are Labeled by Agonists and Discriminated by Antagonists. Mol Pharmacol. 2001;60(4):690–9.

37. Iglesias A, Lage S, Cadavid MI, Loza MI, Brea J. Development of a Multiplex Assay for Studying Functional Selectivity of Human Serotonin 5-HT2A Receptors and Identification of Active Compounds by High-Throughput Screening. J Biomol Screen. 2016;1–8.

38. Knauer CS, Campbell JE, Chio CL FL. Pharmacological characterization of mitogen-activated protein kinase activation by recombinant human 5-HT2C, 5-HT2A, and 5-HT2B receptors. Naunyn Schmiedebergs Arch Pharmacol. 2009;379(5):461–71.

39. Storjohann L, Holst B, Schwartz TW. A second disul de bridge from the N-terminal domain to extracellular loop-2 dampens receptor activity. Biochemistry. 2008;47(35):9198–207.

40. Berg KA, Stout BD, Maayani S, Clarke WP. Differences in rapid desensitization of 5-hydroxytryptamine2A and 5-hydroxytryptamine2C receptor-mediated phospholipase C activation. Pharmacology. 2001;299(2):593–602.

41. Gray JA, Roth BL. Paradoxical trafficking and regulation of 5-HT2A receptors by agonists and antagonists. In: Brain Research Bulletin. 2001. p. 441–51.

42. Scholl DJ, Wells JN. Serine and alanine mutagenesis of the nine native cysteine residues of the human A1 adenosine receptor. Biochem Pharmacol. 2000;60(11):1647–54.

43. Ragnarsson L, Andersson Å, Thomas WG, Lewis RJ. Extracellular surface residues of the α1B-adrenoceptor critical for G protein-coupled receptor function. Mol Pharmacol. 2015;87(1):121–9.

44. Vauquelin G, Van Liefde I, Swinney DC. Radioligand binding to intact cells as a tool for extended drug screening in a representative physiological context. Drug Discov Today Technol. 2015 Oct 1;17:28–34.

45. Rummel PC, Thiele S, Hansen LS, Petersen TP, Sparre-Ulrich AH, Ulven T, et al. Extracellular disulfide bridges serve different purposes in two homologous chemokine receptors, CCR1 and CCR5. Mol Pharmacol. 2013;84(3):335–45.

46. De Filippo E, Namasivayam V, Zappe L, El-Tayeb A, Schiedel AC, Müller CE. Role of extracellular cysteine residues in the adenosine A2A receptor. Purinergic Signal. 2016;12(2):313–29.

47. Guan R, Wu X, Feng X, Zhang M, Hébert TE, Segaloff DL. Structural determinants underlying constitutive dimerization of unoccupied human follitropin receptors. Cell Signal. 2010;22(2):247–56.

48. Naranjo AN, Chevalier A, Cousins GD, Ayettey E, McCusker EC, Wenk C, et al. Conserved disulfide bond is not essential for the adenosine A2A receptor: Extracellular cysteines influence receptor distribution within the cell and ligand-binding recognition. Biochim Biophys Acta - Biomembr. 2015;1848(2):603–14.

49. Herrick-Davis K, Weaver BA, Grinde E, Mazurkiewicz JE. Serotonin 5-HT2C receptor homodimer biogenesis in the endoplasmic reticulum: Real-time visualization with confocal fluorescence resonance energy transfer. J Biol Chem. 2006;281(37):27109–16.

50. Zeng FY, Soldner A, Schöneberg T, Wess J. Conserved extracellular cysteine pair in the M3 muscarinic acetylcholine receptor is essential for proper receptor cell surface localization but not for G protein coupling. J Neurochem. 1999;72(6):2404–14.

51. Glukhova A, Thal DM, Nguyen AT, Vecchio EA, Jörg M, Scammells PJ, et al. Structure of the Adenosine A1 Receptor Reveals the Basis for Subtype Selectivity. Cell. 2017;168(5):867-877.e13.

52. Bruno A, Beato C, Costantino G. Molecular dynamics simulations and docking studies on 3D models of the heterodimeric and homodimeric 5-HT(2A) receptor subtype. Futur Med Chem. 2011;3(6):665–81.

Figure 1. (A) Saturation binding curve of [^{3}H]LSD in the membrane fraction of the WT cell line. The values represent the mean ± SD of one representative experiment carried out in triplicate. (**B**) Specific binding of [^{3}H]LSD in cell membrane fraction of NT cells and the generated mutant cell lines, normalized as the specific binding of each cell line. Each column represents the mean ± SD of three independent experiments carried out in triplicate. ***P < 0.001 (one-way ANOVA followed by Tukey's test).

Figure 2. (A) [^{3}H]LSD binding displacement curve for risperidone in the WT cell line. Each point represents the mean ± SD of three independent experiments carried out in duplicate. (**B**) Specific binding of [^{3}H]LSD in whole cells of NT cells and of the generated mutant cell lines, normalized as the specific binding of each cell line. Each column represents the mean ± SD of three independent experiments carried out in triplicate. **P < 0.01; ***P < 0.001 (one-way ANOVA followed by Tukey's test).

Figure 3. (A) Concentration-response curves elicited by 5-HT, (±)DOI, and LSD, when measuring IPs accumulation in the WT cell line. (**B**) Concentration-response curve for clozapine in the presence of 0.10 μM (±)DOI in the WT cell line. (**C**) Concentration-response curve for haloperidol in the presence of 0.10 μM (±)DOI in the WT cell line. (**D**) IPs accumulation elicited by the agonists 5-HT, (±)DOI, and LSD in C148A, C227A, and C148A/C227A cell lines, compared to WT. Values represent the mean ± SD of three independent experiments carried out in triplicate. ***P < 0.001 (one-way ANOVA followed by Tukey's test).

Figure 4. (A) Concentration-response curves elicited by 5-HT, (±)DOI, and LSD, when measuring calcium mobilization in the WT cell line. (**B**) Concentration-response curve for clozapine in the presence of 0.10 μM (±)DOI in the WT cell line. (**C**) Concentration-response curve for haloperidol in the presence of 0.10 μM (±)DOI in the WT cell line. (**D**) Calcium

mobilization elicited by 1 μM of the agonists 5-HT, (±)DOI, and LSD in C148A, C227A, and C148A/C227A cell lines, compared to WT. (**E**) Calcium mobilization elicited by 100 μM of the agonists 5-HT and (±)DOI in C148A, C227A and C148A/C227A cell lines, compared to WT. Values represent the mean ± SD of three independent experiments carried out in triplicate. ***$P < 0.001$ (one-way ANOVA followed by Tukey's test).

Figure 5. Fluorescence images obtained as a result of staining the cell lines expressing the WT 5-HT_{2A} receptor (**A**), and the mutated C148A (**B**), C227A (**C**), and C148A/C227A (**D**) 5-HT_{2A} receptors. The nucleus is stained in blue, the endoplasmic reticulum is stained in red, and the receptor is represented in green. Representative microphotographs obtained out of six independent experiments carried out in septuplicate.

Figure 6. Fluorescence intensity of YFP measured in whole cells expressing WT, C148A, C227A, and C148A/C227A receptors. Each column represents the mean ± SD of at least six experiments carried out in septuplicate. . *$P < 0.05$; ***$P < 0.001$ (one-way ANOVA followed by Tukey's test).

Figure 7. (**A**) Fluorescence measurements of YFP in the cell membrane of cells expressing WT, C148A, C227A, and C148A/C227A receptors. Each column represents the mean ± SD of at least six experiments carried out in septuplicate. (**B**) Fluorescence measurements of Alexa 627 fluorescence intensity (receptor) related to Alexa 555 fluorescence intensity (plasma membrane) of cells expressing WT, C148A, C227A and C148A/C227A receptors. Each column represents the mean ± SD of one representative experiment carried out in twelve identical points. *$P < 0.05$; **$P < 0.01$; ***$P < 0.001$ (one-way ANOVA followed by Tukey's test).

Figure 8. Fluorescence intensity in the reticulum, represented as the ratio of YFP measurements in the reticulum and YFP measurements in whole cells expressing the WT,

C148A, C227A, and C148A/C227A receptors. Each column represents the mean ± SD of at least six experiments carried out in septuplicate. *$P < 0.05$; **$P < 0.01$; ***$P < 0.001$ (one-way ANOVA followed by Tukey's test).

Figure 9. (A) BRET saturation curves for the WT 5-HT_{2A} receptor (black line) or the mutated receptors (C148A, red line; C227A, blue line; C148A/C227A, green line) in transiently transfected HEK293T/17 cells. Cells were co-transfected with a fixed amount of Rluc-N2-5-GPCR and increasing amounts of pcDNA3-GPCR-eYFP. The graph shows the results (expressed as the mean ± SD) of one representative experiment out of three, performed in quadruplicate. (**B**) Values of $BRET_{max}$ obtained after transfecting with 100 ng or 150 ng DNA per well, compared to the WT receptor. (**C**) Receptor expression measurements after transfecting with 100 ng or 150 ng DNA per well, compared to the WT receptor. The data is from one representative experiment carried out in quadruplicate. *$P < 0.05$; **$P < 0.01$; ***$P < 0.001$ (one-way ANOVA followed by Tukey's test).

Figure 10. (**A**) Western blot image obtained from cell lysates of the NT, WT, C148A, C227A, and C148A/C227A cell lines. One representative image is shown from three independent experiments (**B**) Protein expression quantified by densitometric analysis with Image J, and expressed as the ratio dimer/monomer. Columns represent the mean ± SD of three independent experiments.

Figure 11. Representation of 5-HT_{2A} receptor with the C148A, C227A, and C148A/C227A substitutions. Extracellular cysteines are indicated in orange; the alanine substitutions are indicated in blue. Orange arrows represent the interaction possibilities of free extracellular cysteines.

Essential role of the C148 – C227 disulphide bridge in the human 5-HT_{2A} homodimeric receptor

Table 1. Amino acid sequences of the critical region of the coding plasmid of the human (WT) and mutant 5-HT_{2A} constructs.

	TM-3	ECL-2
WT plasmid	GYRWPLPSKL**C**AVWIYLDVLF 138 158	DDSKVFKEGS**C**LLADDNFVLI 217 237
C148A plasmid	GYRWPLPSKL**A**AVWIYLDVLF 138 158	DDSKVFKEGS**C**LLADDNFVLI 217 237
C227A plasmid	GYRWPLPSKL**C**AVWIYLDVLF 138 158	DDSKVFKEGS**A**LLADDNFVLI 217 237
C148A/C227A plasmid	GYRWPLPSKL**A**AVWIYLDVLF 138 158	DDSKVFKEGS**A**LLADDNFVLI 217 237

Table 2. Potency (pEC_{50}) and efficacy (% E_{max}) of 5-HT, (±)DOI, and LSD, to IPs accumulation in the WT cell line. Values represent the mean ± SD of two independent experiments carried out in triplicate.

	pEC_{50}	**% E_{max} (100 µM 5-HT)**
5-HT	7.80 ± 0.05	101.10 ± 1.36
(±)DOI	7.44 ± 0.27	40.12 ± 3.82
LSD	9.36 ± 0.37	25.79 ± 2.65

Table 3. Potency (pEC_{50}) and efficacy (% E_{max}) of 5-HT, (±)DOI, and LSD, to calcium in the WT cell line. Values represent the mean ± SD of three independent experiments carried out in triplicate.

	pEC_{50}	**% E_{max} (10 µM 5-HT)**
5-HT	7.22 ± 0.29	96.66 ± 11.91
(±)DOI	7.86 ± 0.17	61.88 ± 4.14
LSD	7.72 ± 0.17	51.07 ± 4.34

Essential role of the C148 – C227 disulphide bridge in the human 5-HT_{2A} homodimeric receptor

Figure 1A

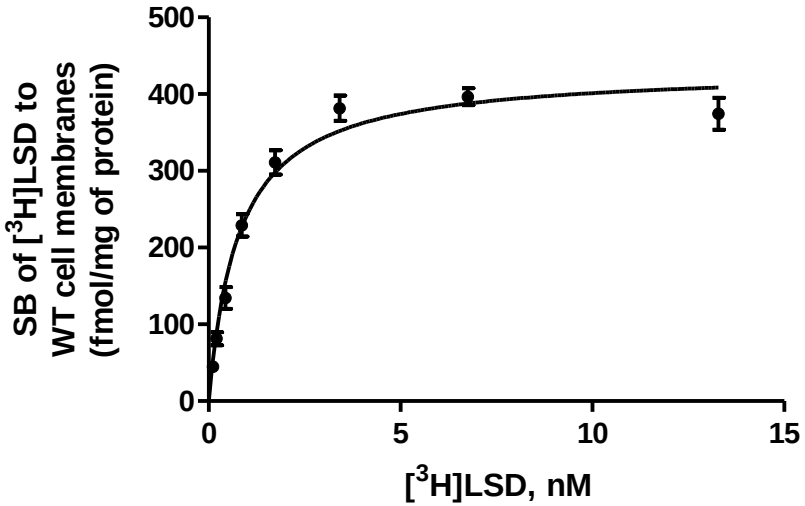

Essential role of the C148 – C227 disulphide bridge in the human 5-HT_{2A} homodimeric receptor

Figure 2A

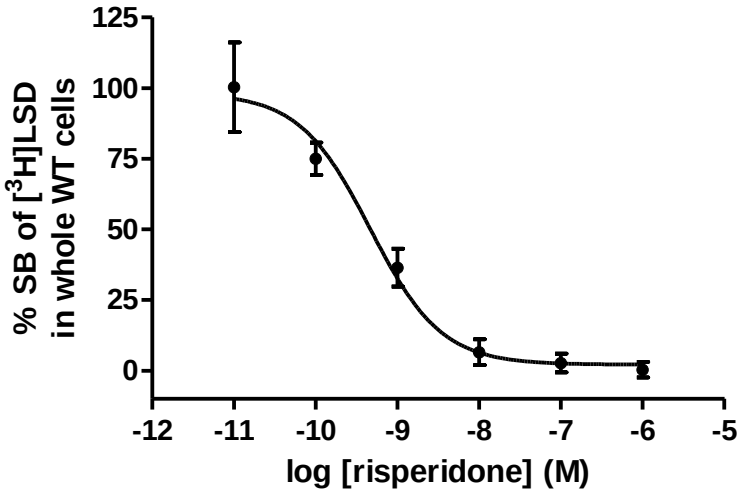

Essential role of the C148 – C227 disulphide bridge in the human 5-HT_{2A} homodimeric receptor

Figure 1B

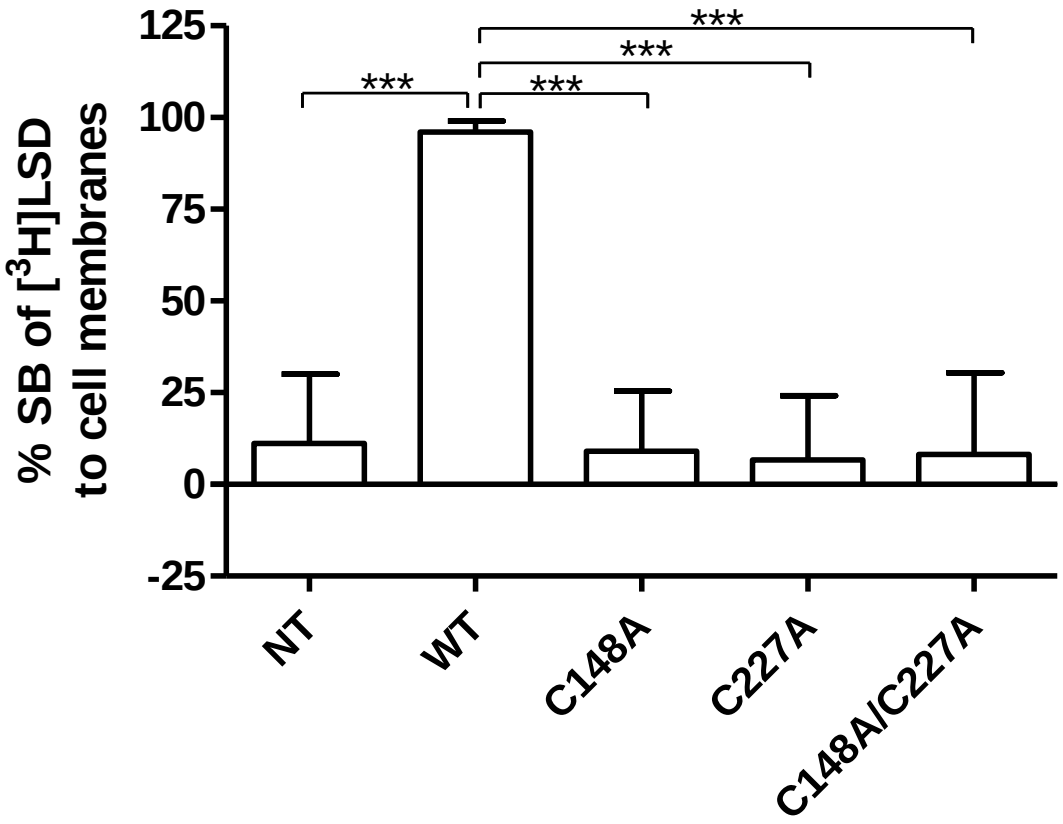

Essential role of the C148 – C227 disulphide bridge in the human 5-HT_{2A} homodimeric receptor

Figure 2B

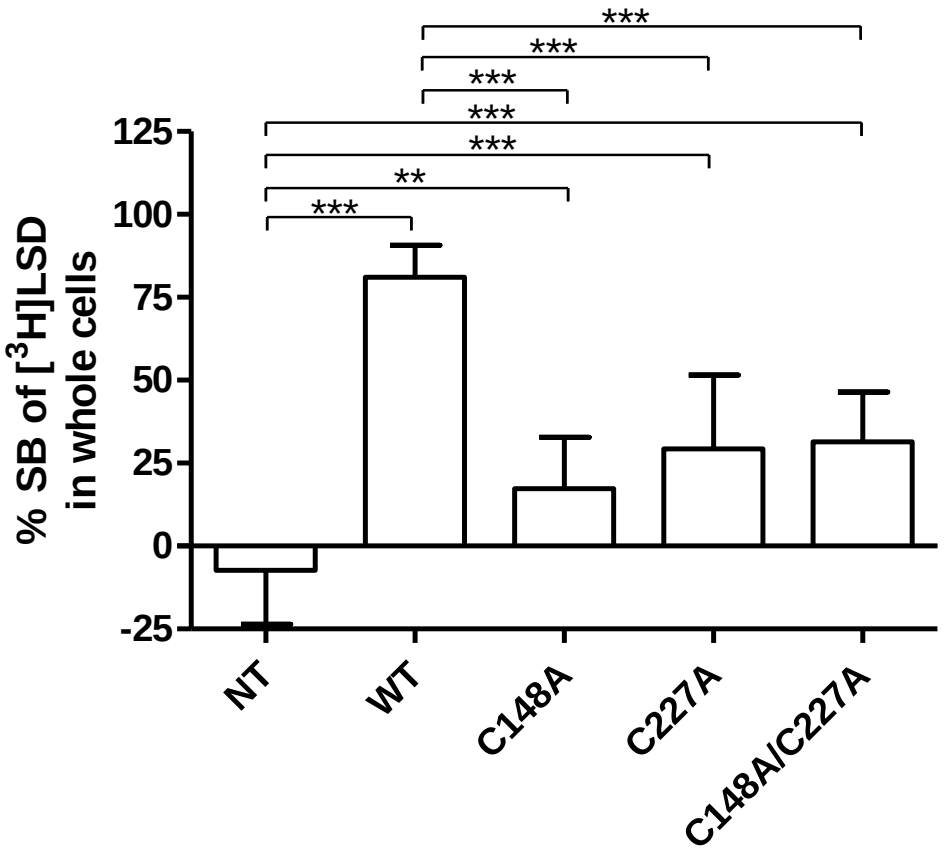

Essential role of the C148 – C227 disulphide bridge in the human 5-HT_{2A} homodimeric receptor

Figure 3A

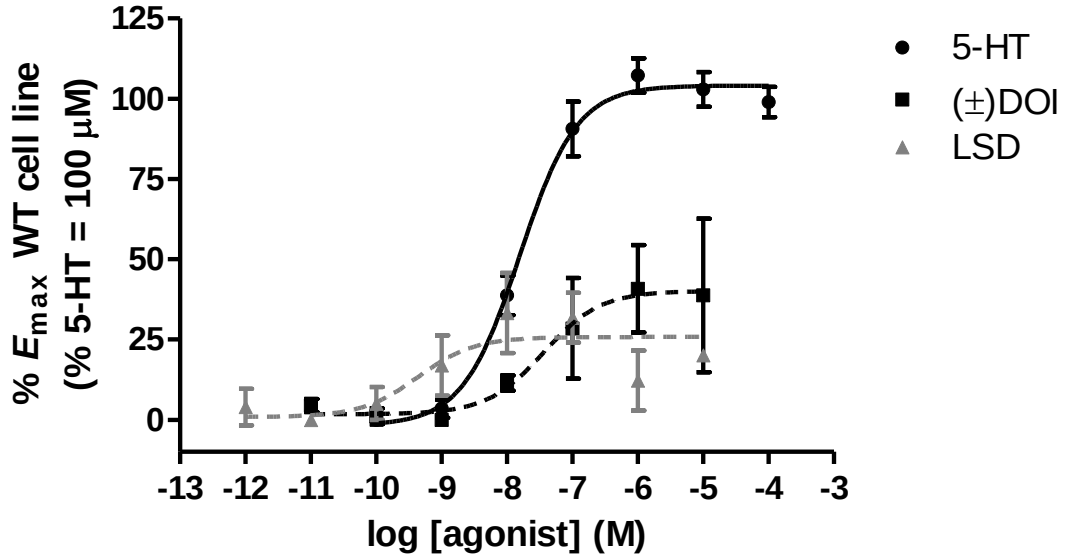

Essential role of the C148 – C227 disulphide bridge in the human 5-HT_{2A} homodimeric receptor

Figure 3B

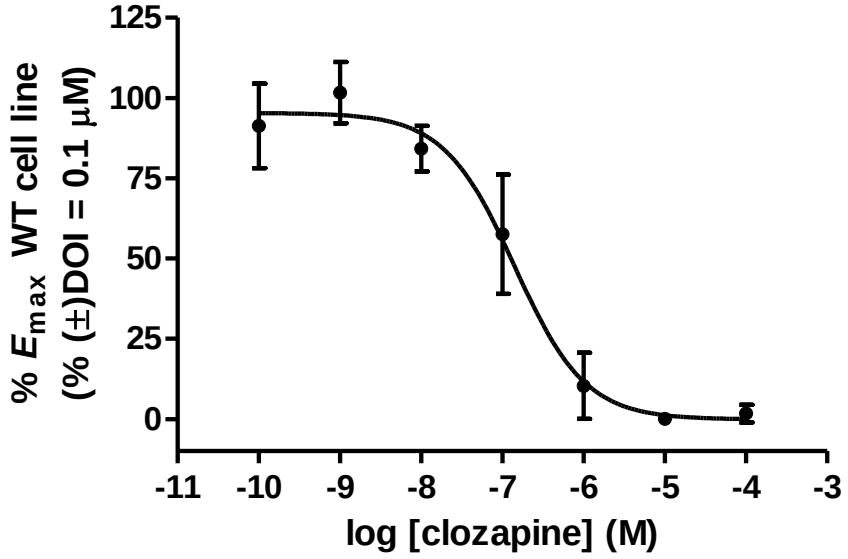

Essential role of the C148 – C227 disulphide bridge in the human 5-HT_{2A} homodimeric receptor

Figure 3C

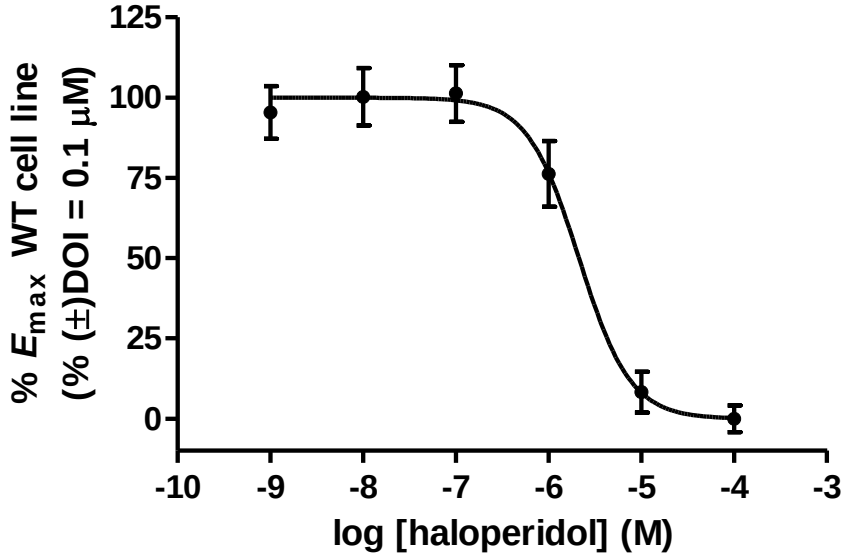

Essential role of the C148 – C227 disulphide bridge in the human 5-HT_{2A} homodimeric receptor

Figure 3D

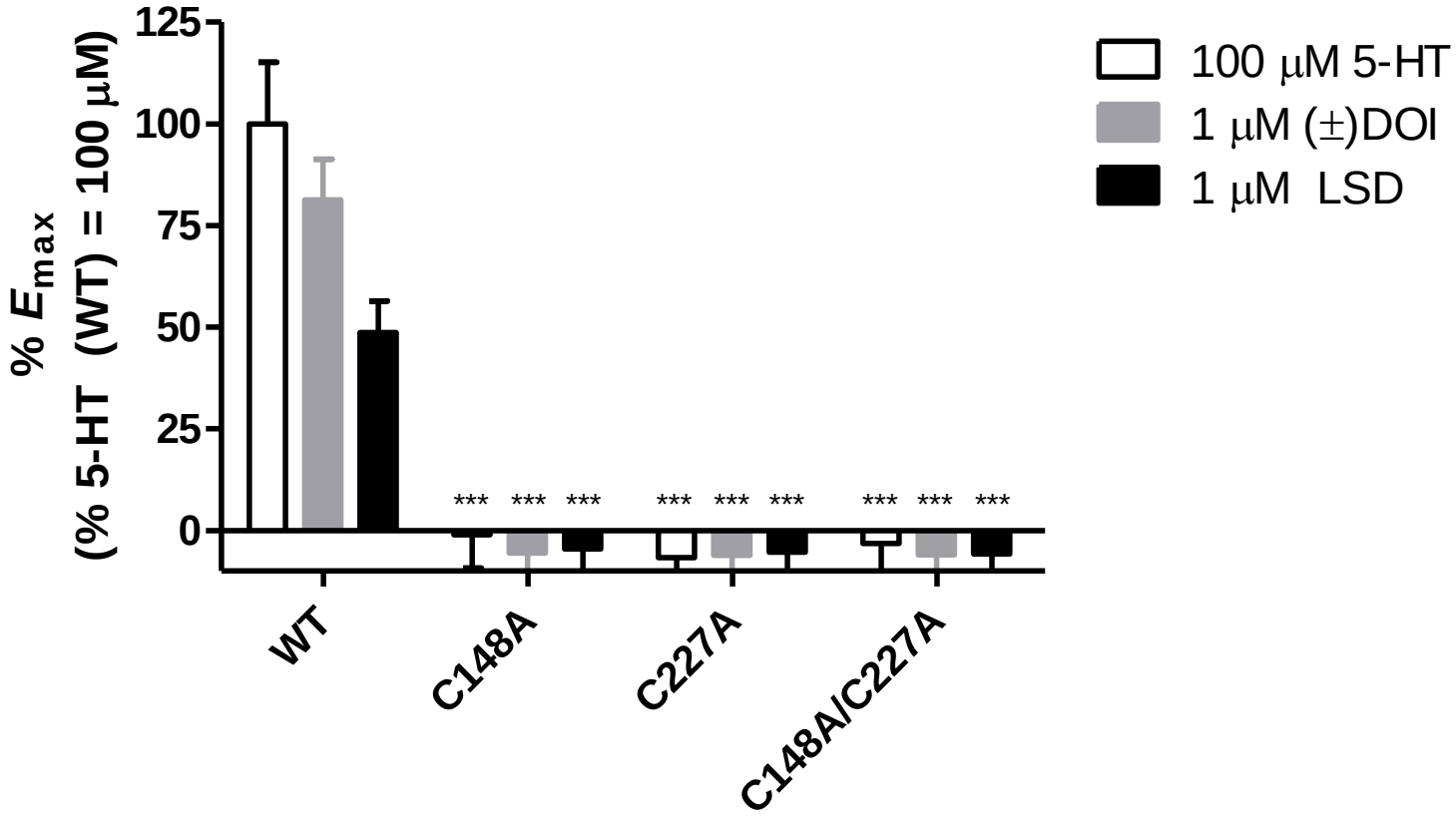

Essential role of the C148 – C227 disulphide bridge in the human 5-HT_{2A} homodimeric receptor

Figure 4A

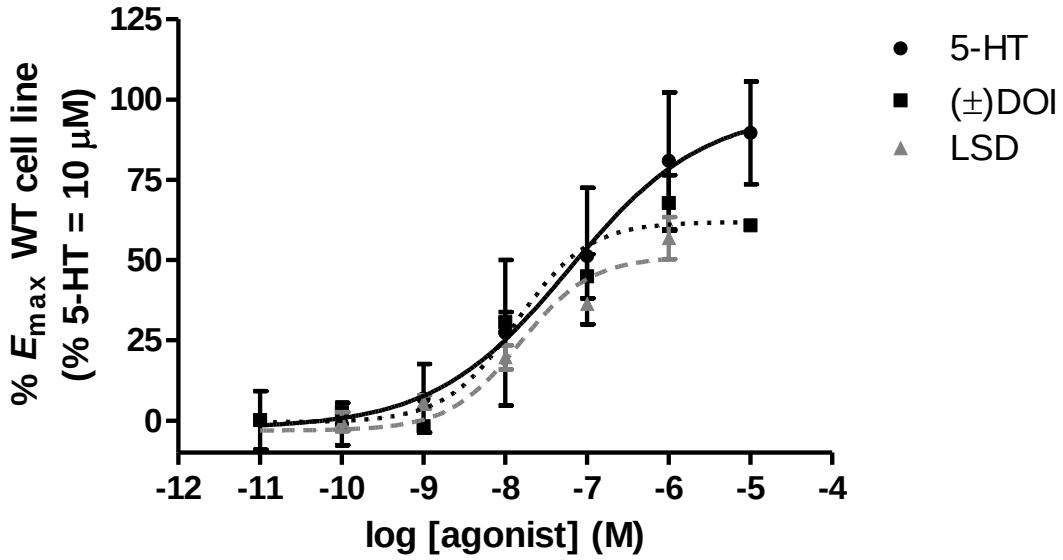

Essential role of the C148 – C227 disulphide bridge in the human 5-HT_{2A} homodimeric receptor

Figure 4B

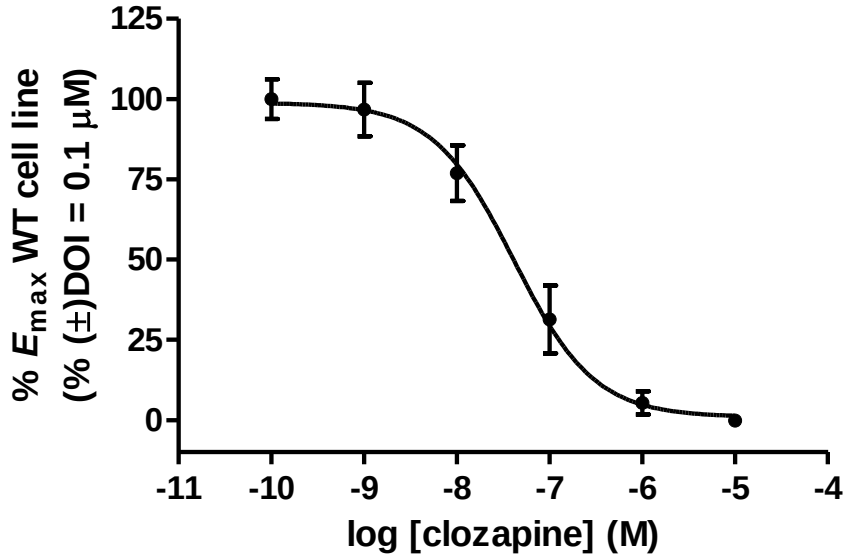

Essential role of the C148 – C227 disulphide bridge in the human 5-HT_{2A} homodimeric receptor

Figure 4C

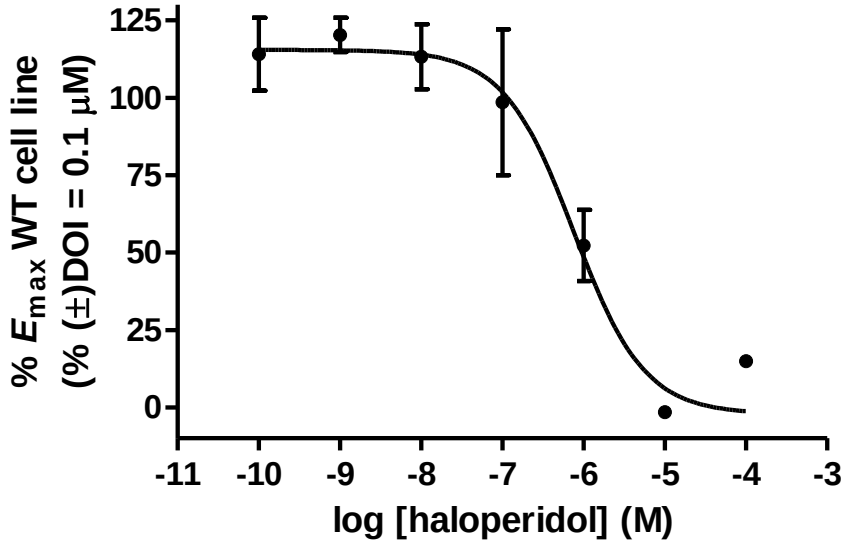

Essential role of the C148 – C227 disulphide bridge in the human 5-HT_{2A} homodimeric receptor

Figure 4D

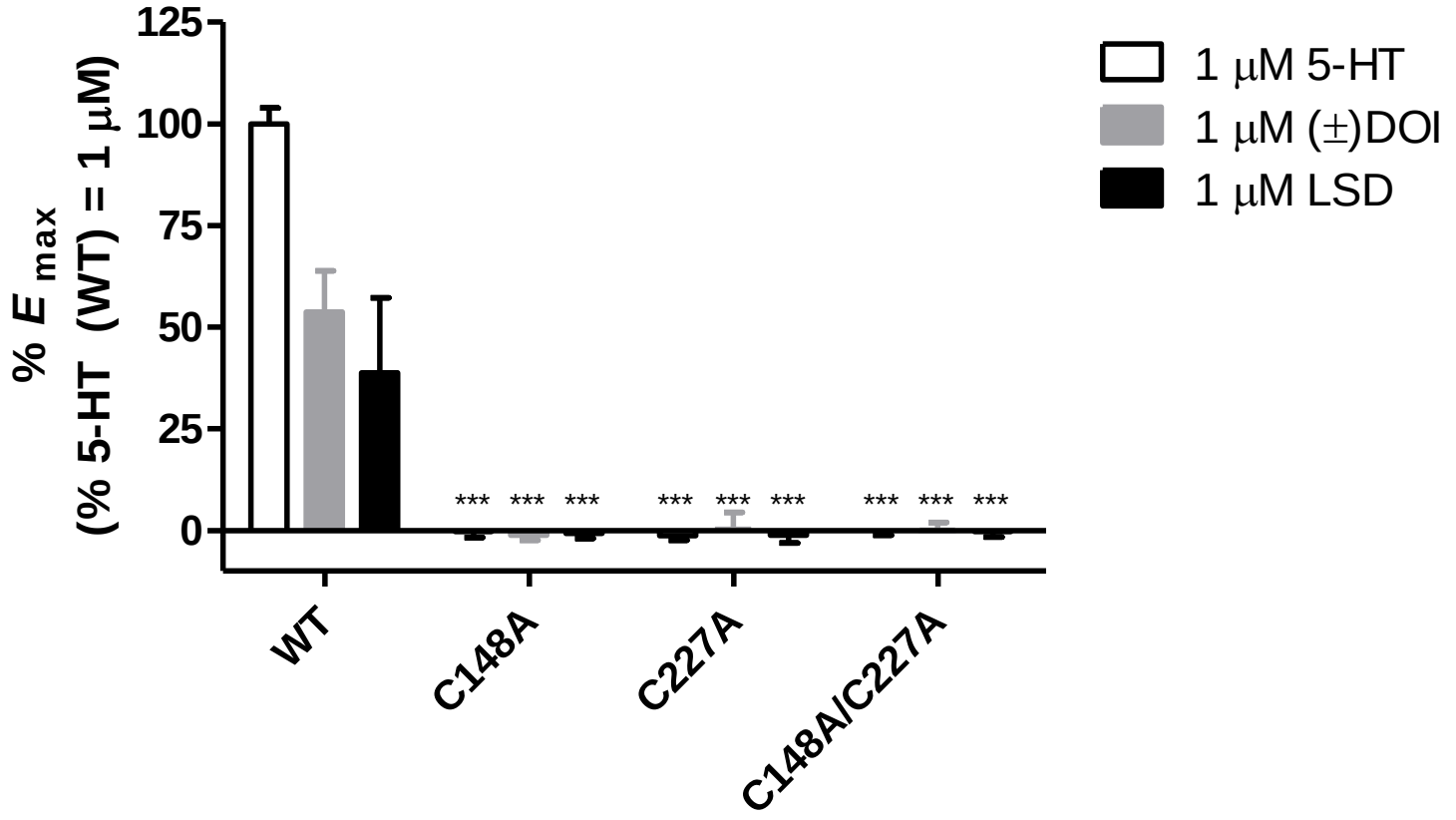

Essential role of the C148 – C227 disulphide bridge in the human 5-HT$_{2A}$ homodimeric receptor

Figure 4E

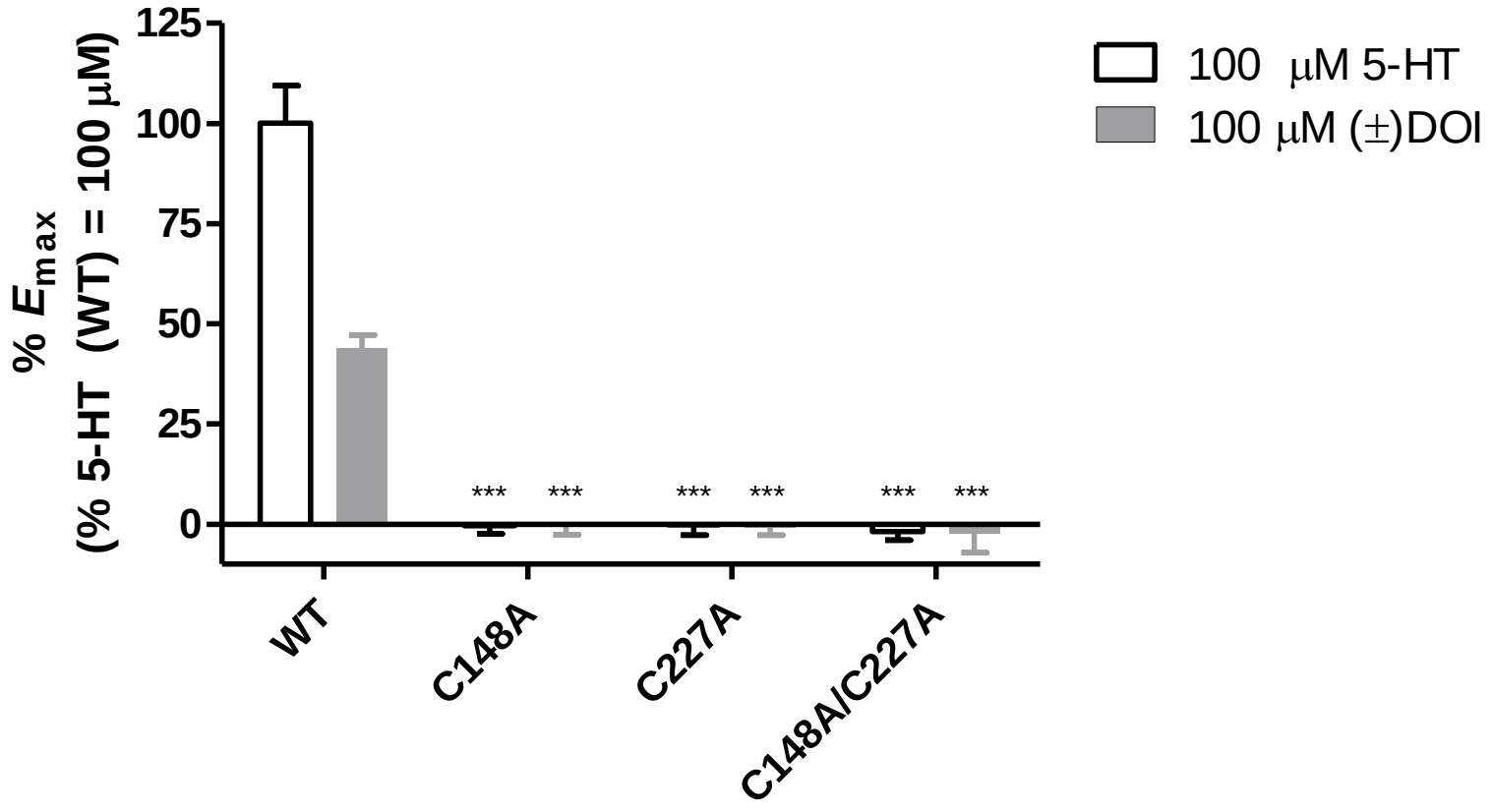

Essential role of the C148 – C227 disulphide bridge in the human 5-HT_{2A} homodimeric receptor

Figure 5A

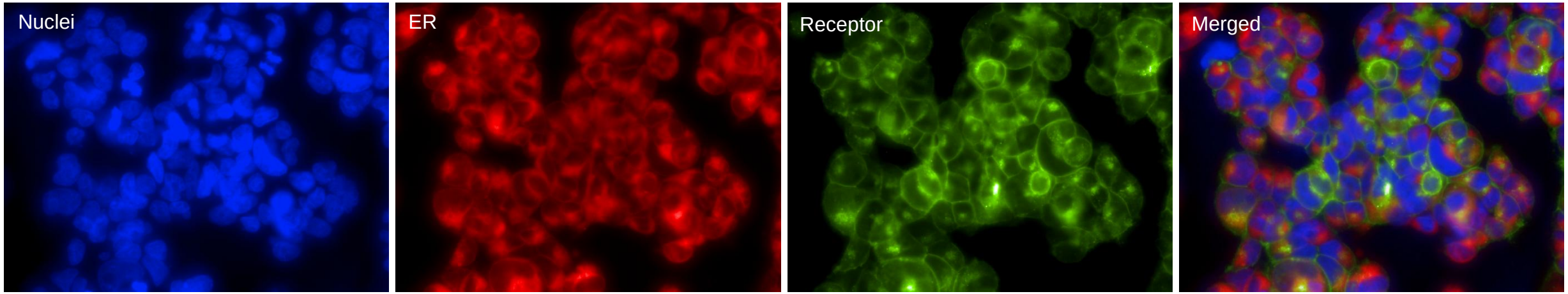

Essential role of the C148 – C227 disulphide bridge in the human 5-HT_{2A} homodimeric receptor

Figure 5B

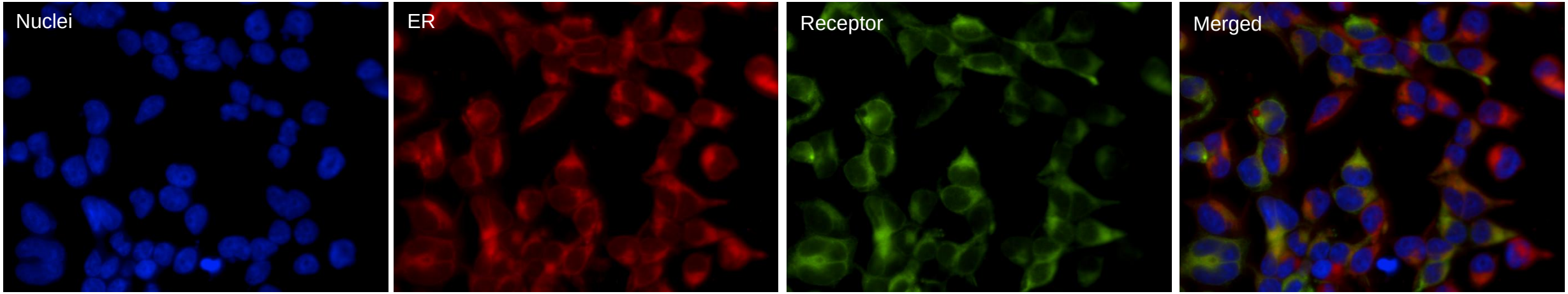

Essential role of the C148 – C227 disulphide bridge in the human 5-HT_{2A} homodimeric receptor

Figure 5C

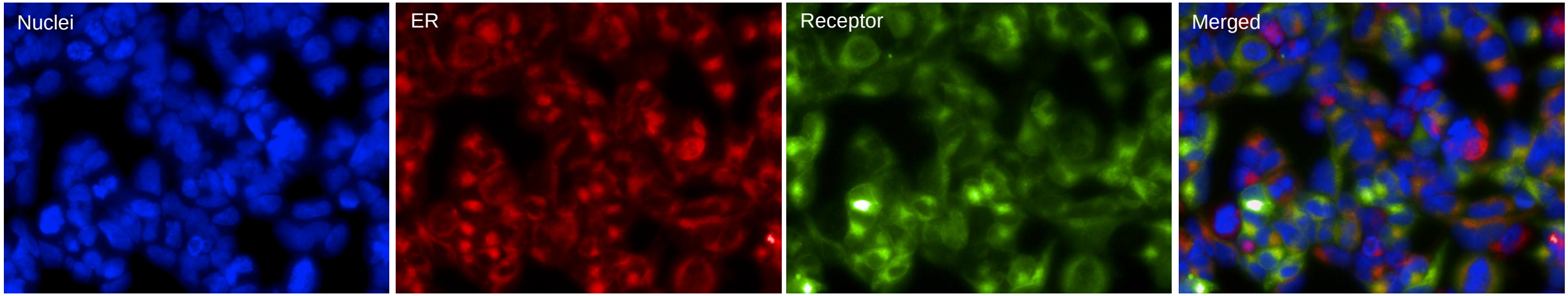

Essential role of the C148 – C227 disulphide bridge in the human 5-HT_{2A} homodimeric receptor

Figure 5D

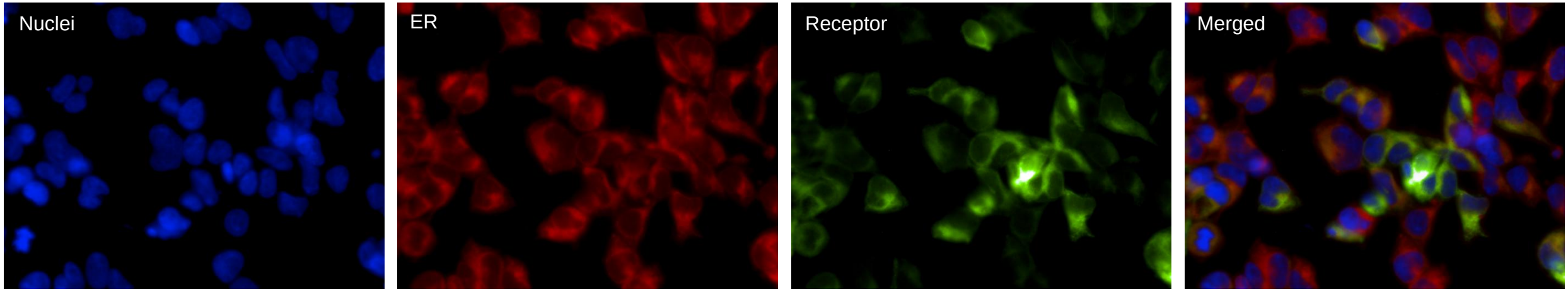

Essential role of the C148 – C227 disulphide bridge in the human 5-HT_{2A} homodimeric receptor

Figure 6

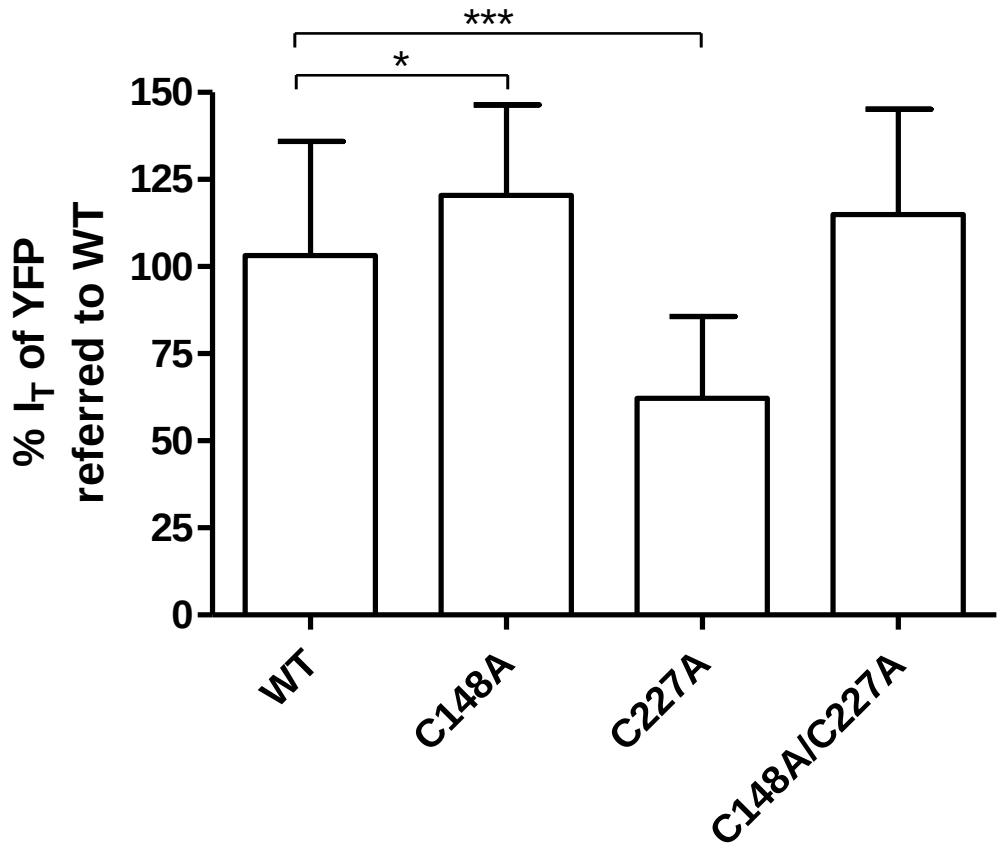

Essential role of the C148 – C227 disulphide bridge in the human 5-HT_{2A} homodimeric receptor

Figure 7A

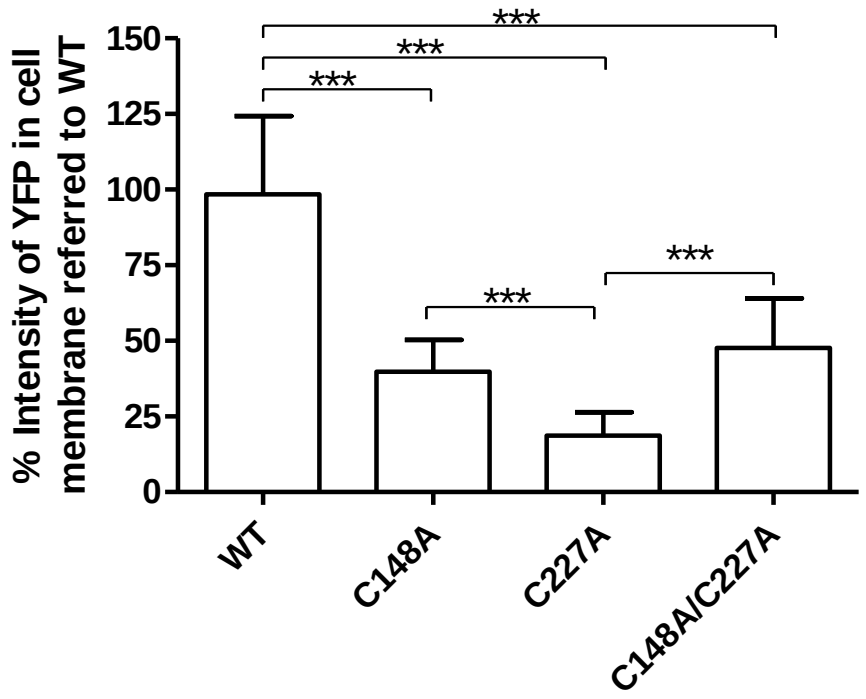

Essential role of the C148 – C227 disulphide bridge in the human 5-HT_{2A} homodimeric receptor

Figure 7B

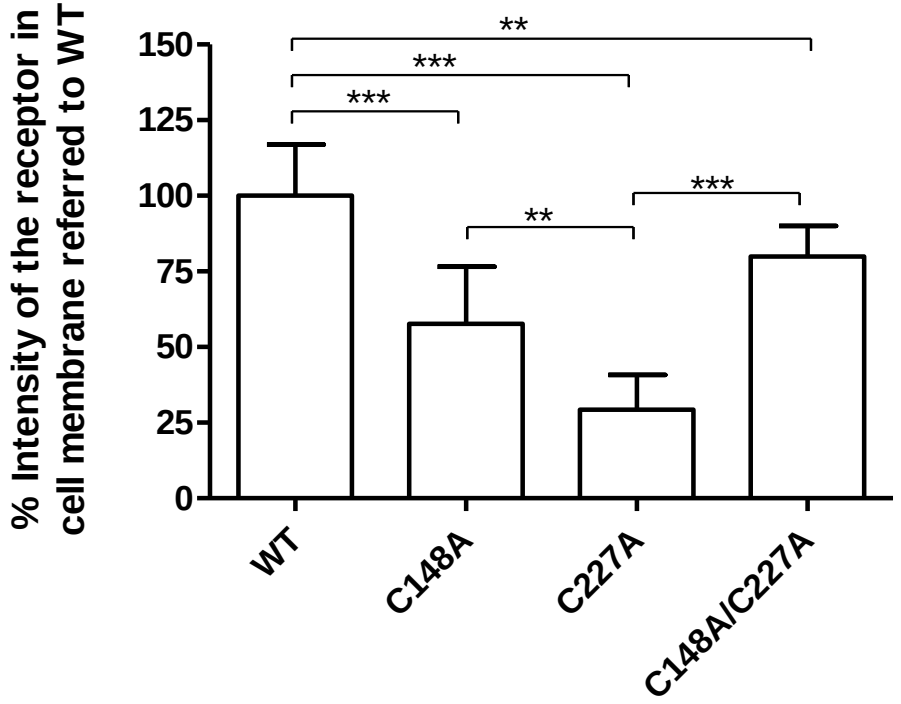

Essential role of the C148 – C227 disulphide bridge in the human 5-HT_{2A} homodimeric receptor

Figure 8

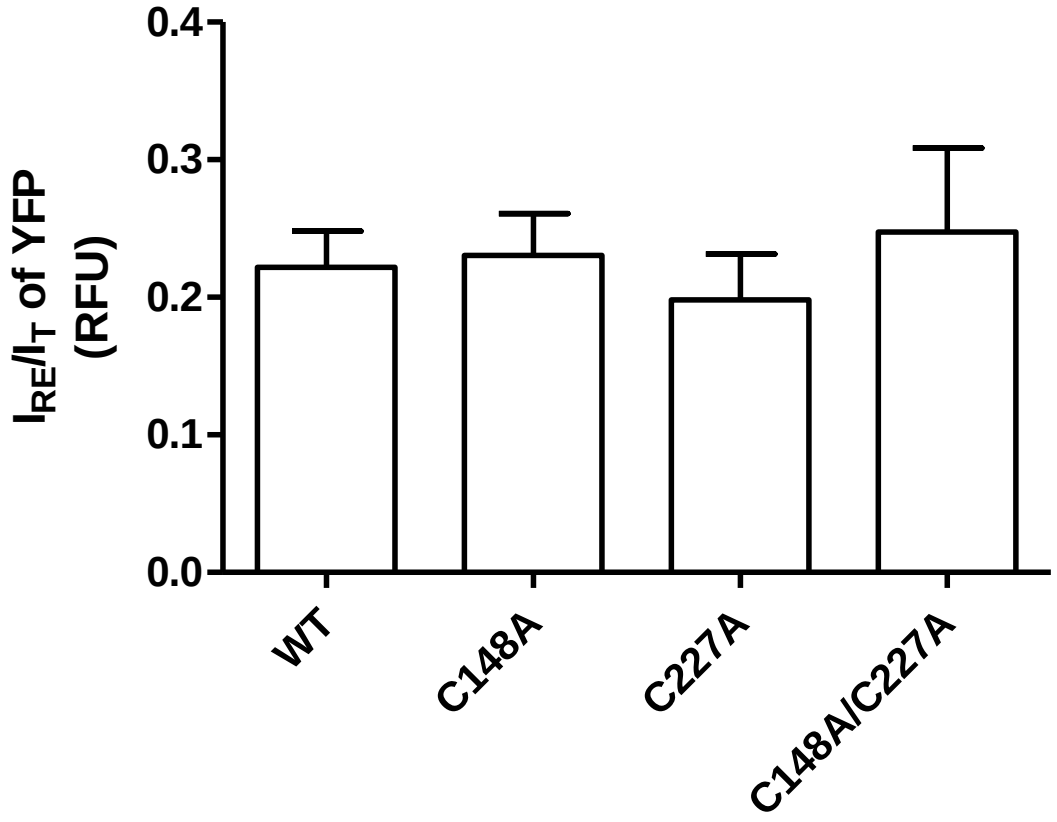

Essential role of the C148 – C227 disulphide bridge in the human 5-HT_{2A} homodimeric receptor

Figure 9A

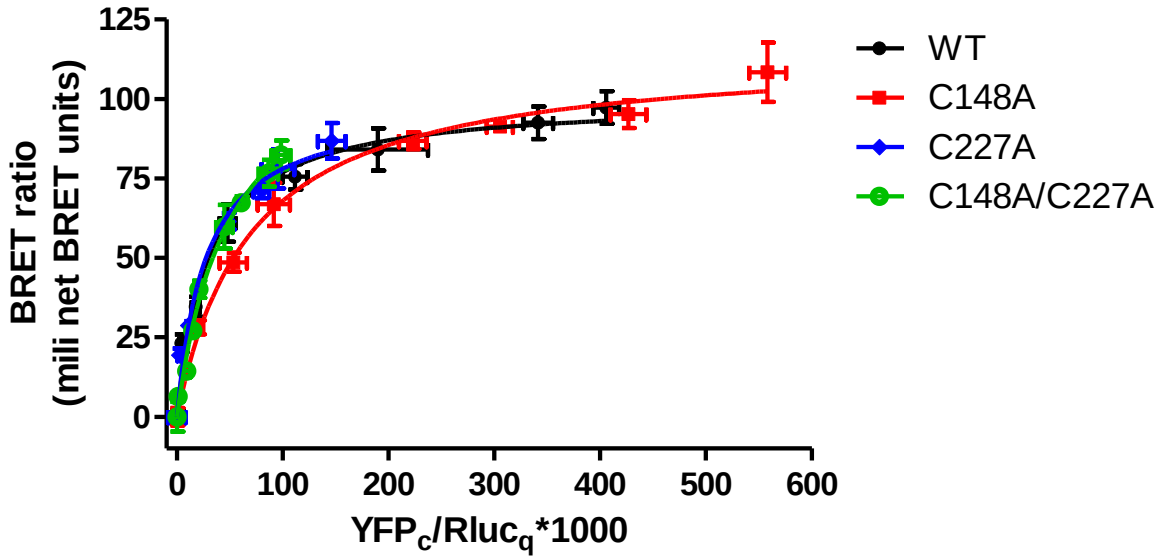

Essential role of the C148 – C227 disulphide bridge in the human 5-HT_{2A} homodimeric receptor

Figure 9B

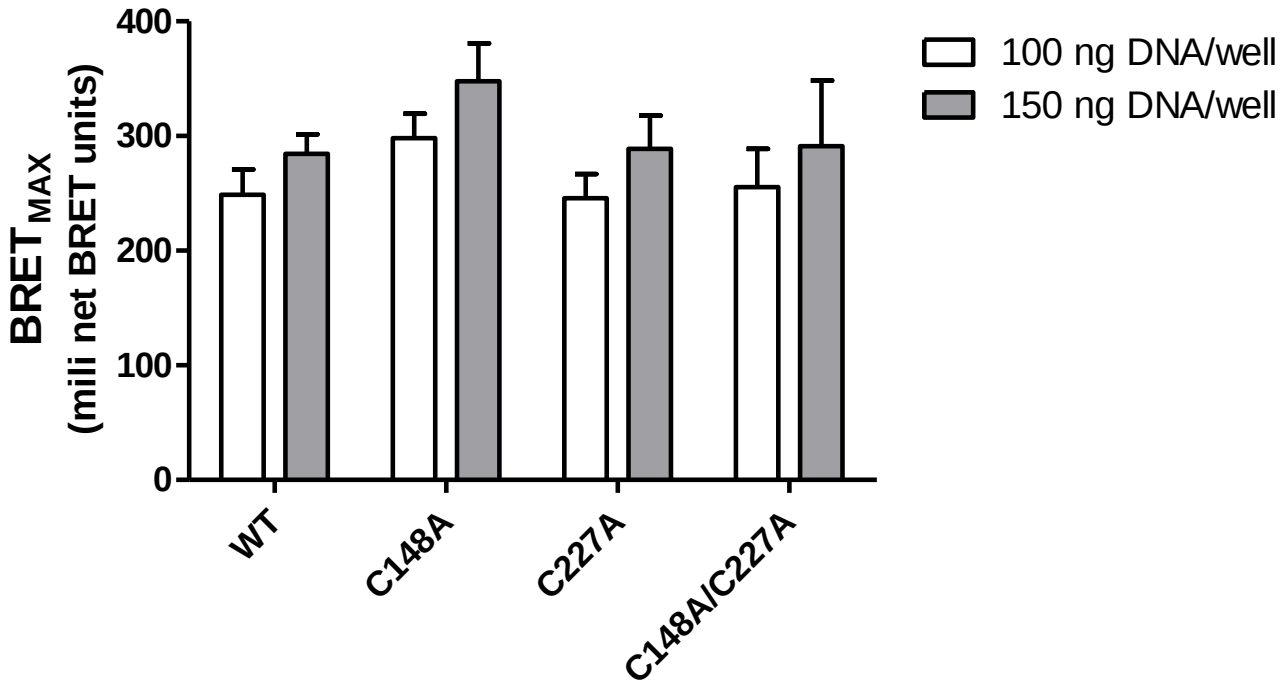

Essential role of the C148 – C227 disulphide bridge in the human 5-HT_{2A} homodimeric receptor

Figure 9C

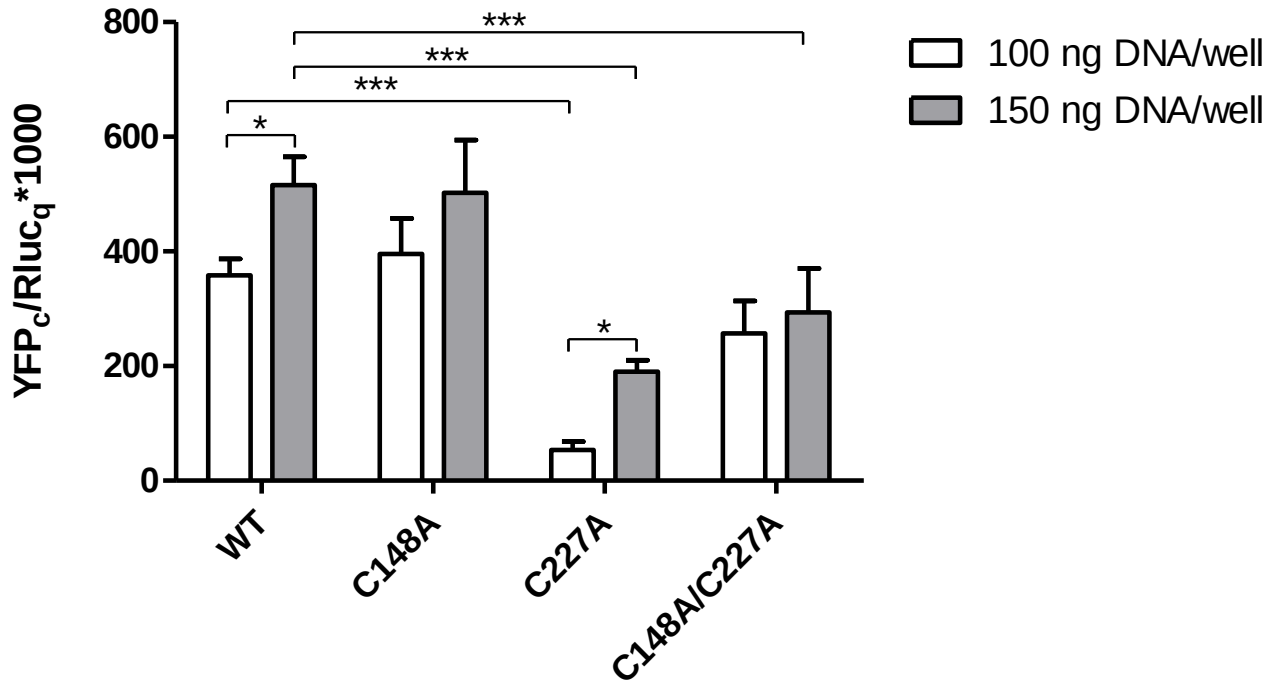

Essential role of the C148 – C227 disulphide bridge in the human 5-HT_{2A} homodimeric receptor

Figure 10A

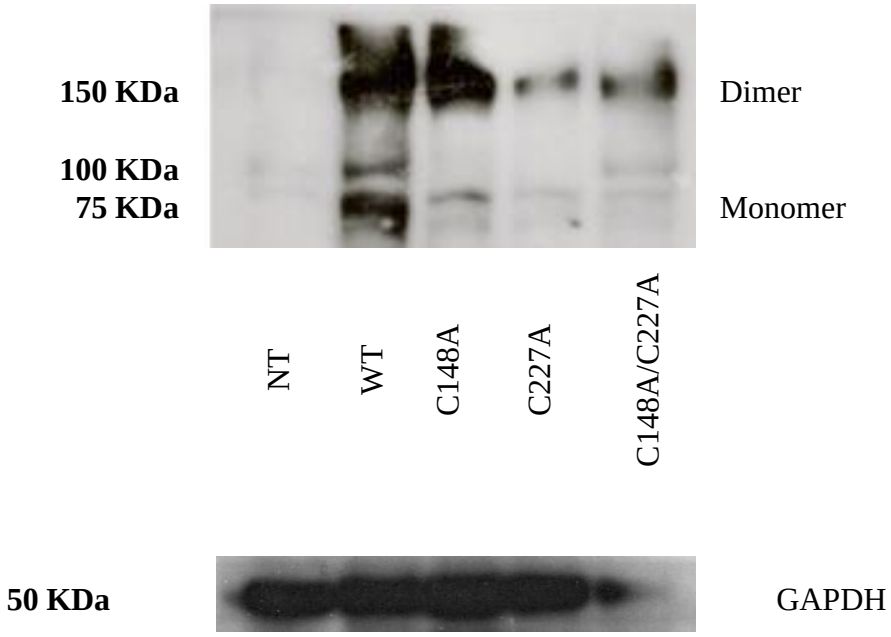

Essential role of the C148 – C227 disulphide bridge in the human 5-HT_{2A} homodimeric receptor

Figure 10B

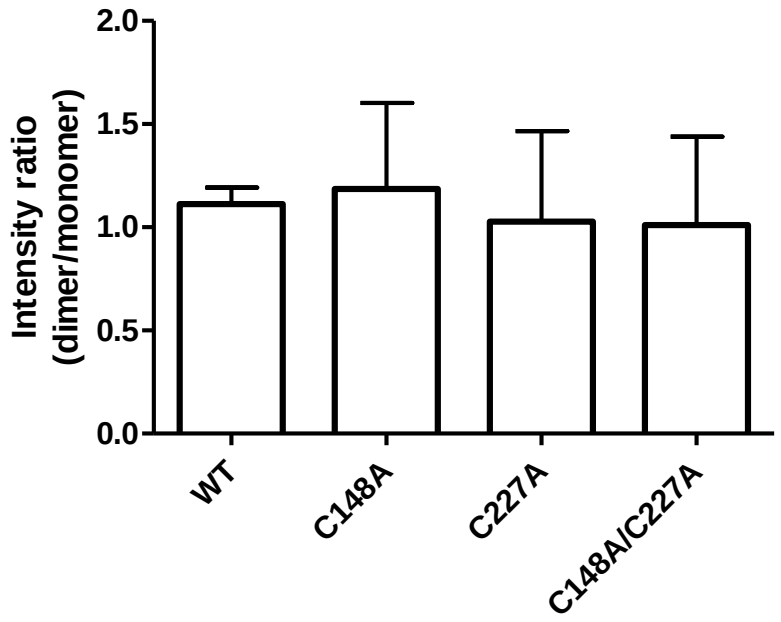

Essential role of the C148 – C227 disulphide bridge in the human 5-HT_{2A} homodimeric receptor

Figure 11

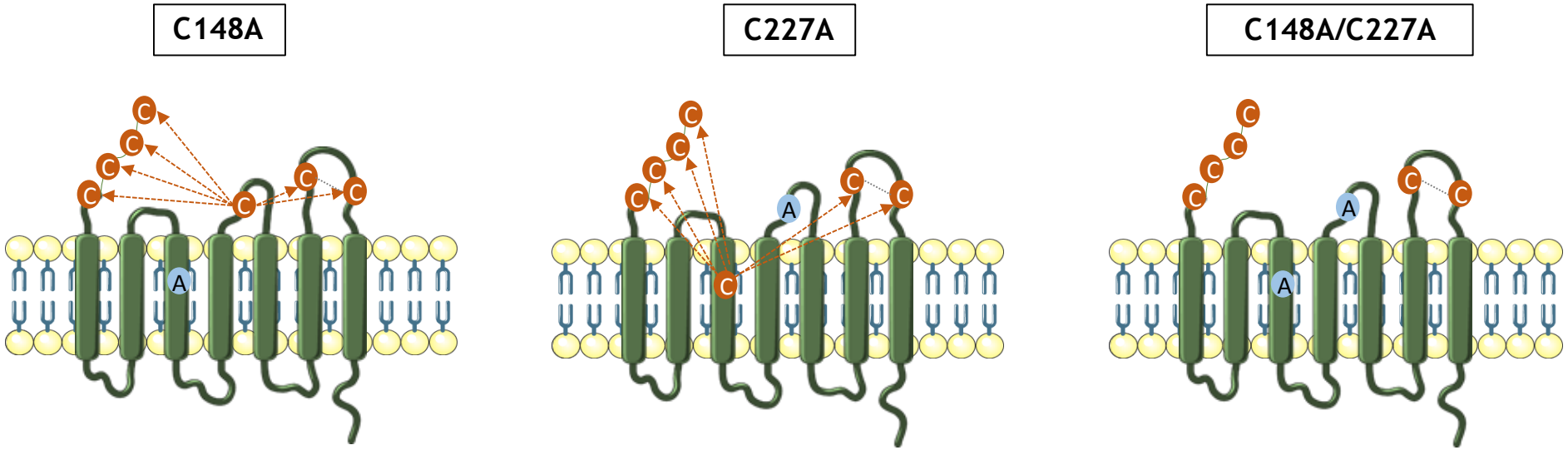

*Graphical Abstract (for review)

Click here to download high resolution image